

QC  
807.5  
.U66  
no.216

NOAA TR ERL 216-WPL 17

# NOAA Technical Report ERL 216-WPL 17

U.S. DEPARTMENT OF COMMERCE  
National Oceanic and Atmospheric Administration  
Environmental Research Laboratories

## Acoustic Echo Sounding as Related to Air Pollution in Urban Environments

W. R. SIMMONS

J. W. WESCOTT

F. F. HALL, JR.

BOULDER, COLO.  
MAY 1971





## ENVIRONMENTAL RESEARCH LABORATORIES

One of the Environmental Research Laboratories is to study the oceans, inland water and upper atmosphere, the space environment, and the earth, in search of understanding needed to provide more useful services in improving man's prospects as influenced by the physical environment. Laboratories contributing to these

**Earth Sciences Laboratories (ESL):** Geomagnetism, seismology, geodesy, and related sciences; earthquake processes, internal structure and accurate figure of the Earth, and distribution of the Earth's mass.

**Atlantic Oceanographic and Meteorological Laboratories (AOML):** Oceanography, with emphasis on the geology and geophysics of ocean basins, oceanic processes, sea-air interactions, hurricane research, and weather modification (Miami, Florida).

**Pacific Oceanographic Laboratories (POL):** Oceanography; geology and geophysics of the Pacific Basin and margins; oceanic processes and dynamics; tsunami generation, propagation, modification, detection, and monitoring (Seattle, Washington).

**Atmospheric Physics and Chemistry Laboratory (APCL):** Cloud physics and precipitation; chemical composition and nucleating substances in the lower atmosphere; and laboratory and field experiments toward developing feasible methods of weather modification.

**Air Resources Laboratories (ARL):** Diffusion, transport, and dissipation of atmospheric contaminants; development of methods for prediction and control of atmospheric pollution (Silver Spring, Maryland).

**Geophysical Fluid Dynamics Laboratory (GFDL):** Dynamics and physics of geophysical fluid systems; development of a theoretical basis, through mathematical modeling and computer simulation, for the behavior and properties of the atmosphere and the oceans (Princeton, New Jersey).

**Research Flight Facility (RFF):** Outfits and operates aircraft specially instrumented for research; and meets needs of NOAA and other groups for environmental measurements for aircraft (Miami, Florida).

**National Severe Storms Laboratory (NSSL):** Tornadoes, squall lines, thunderstorms, and other severe local convective phenomena toward achieving improved methods of forecasting, detecting, and providing advance warnings (Norman, Oklahoma).

**Space Environment Laboratory (SEL):** Conducts research in solar-terrestrial physics, provides services and technique development in areas of environmental monitoring, forecasting, and data archiving.

**Aeronomy Laboratory (AL):** Theoretical, laboratory, rocket, and satellite studies of the physical and chemical processes controlling the ionosphere and exosphere of the earth and other planets.

**Wave Propagation Laboratory (WPL):** Development of new methods for remote sensing of the geophysical environment; special emphasis on propagation of sound waves, and electromagnetic waves at millimeter, infrared, and optical frequencies.

**Marine Minerals Technology Center (MMTC):** Research into aspects of undersea mining of hard minerals; development of tools and techniques to characterize and monitor the marine mine environment; prediction of the possible effects of marine mining on the environment; development of fundamental mining technology (Tiburon, California).

## NATIONAL OCEANIC AND ATMOSPHERIC ADMINISTRATION

BOULDER, COLORADO 80302





U.S. DEPARTMENT OF COMMERCE

Maurice H. Stans, Secretary

NATIONAL OCEANIC AND ATMOSPHERIC ADMINISTRATION

Robert M. White, Administrator

ENVIRONMENTAL RESEARCH LABORATORIES

Wilmot N. Hess, Director

QC  
807.5  
-466  
no. 216

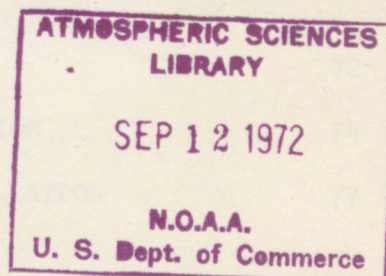
## NOAA TECHNICAL REPORT ERL 216-WPL 17

# Acoustic Echo Sounding as Related to Air Pollution in Urban Environments

W. R. SIMMONS

J. W. WESCOTT

F. F. HALL, JR.



BOULDER, COLO.

May 1971

For sale by the Superintendent of Documents, U. S. Government Printing Office, Washington, D. C. 20402  
Price 75 cents

'72 4914 1



## DISCLAIMER

The Environmental Research Laboratories, National Oceanic and Atmospheric Administration, U.S. Department of Commerce, does not approve, recommend or endorse any proprietary product or proprietary material mentioned in this publication. No reference shall be made to the Environmental Research Laboratories, or to this publication furnished by the Environmental Research Laboratories, in an advertising or sales promotion which would indicate or imply that the Environmental Research Laboratories approves, recommends or endorses any proprietary product or proprietary material mentioned herein, or which has as its purpose an intent to cause directly or indirectly the advertised product to be used or purchased because of this Environmental Research Laboratories publication.

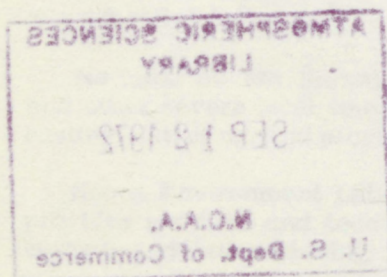




# TABLE OF CONTENTS

	Page
ABSTRACT	1
1. INTRODUCTION	1
2. PHASE I - SYSTEM ANALYSIS OF THE OPERATION OF ACOUSTIC SOUNDERS	3
2.1 Environmental Noise Levels	3
2.2 Environmental Noise Received by the Acoustic Antenna	5
2.3 The Effects of Acoustic Power Radiated in Side Lobes	16
2.4 An Estimate of Useable Acoustic Frequencies	31
2.5 Conclusions on the Operability of Acoustic Sounders	36
3. PHASE II - ECHO SOUNDER DESIGN AND EXPERIMENTAL RESULTS	40
3.1 WPL Mark II Echo Sounder	41
3.2 Sidelobe Radiation	51
3.3 Echo Signals and Ambient Noise Levels	54
3.3.1 Meteorological Conditions	56
3.3.2 Location	57
3.3.3 Antenna Characteristics	58
3.3.4 Carrier Frequency	65
3.3.5 Pulse Length-Receiver Bandwidth	66
3.3.6 Radiated Acoustic Power	67
4. CONCLUSIONS	70
5. ACKNOWLEDGMENTS	71
6. REFERENCES	72
APPENDIX A - DERIVATION OF THE NOISE FIGURE EQUATION	74
APPENDIX B - DERIVATION OF THE ISOLATION RADIUS EQUATION	77



# ACOUSTIC ECHO SOUNDING AS RELATED TO AIR POLLUTION IN URBAN ENVIRONMENTS

W. R. Simmons, J. W. Wescott, and F. F. Hall, Jr.

The feasibility of operating an acoustic echo sounder in an urban or industrial environment, without serious degradation in performance and without contributing to noise pollution, is confirmed. Anechoic absorbers placed about the acoustic antenna are the key to improving the sounder performance. Optimum operating frequencies are between 1 and 2 kHz. The design and operation of the all solid state circuitry is described.

Key words: Atmospheric acoustics, acoustic echo sounder, urban noise

## 1. INTRODUCTION

The acoustic echo sounder has demonstrated its capability for detecting temperature inversions, thermal structure variability, and turbulence in the atmospheric boundary layer (Little, 1969; McAllister, et al., 1969). Requirements exist for improved methods of monitoring these atmospheric parameters in air pollution control work in urban environments. This study was undertaken to determine if an acoustic echo sounder might be feasible as a routine tool for the air quality meteorologist.

Two phases of the study are reported here. Phase I was a system analysis using existing information to determine: (a) the effects of ambient environmental noise on the receiving sensitivity of the echo sounder, (b) the operating conditions necessary to allow the echo sounder to transmit an acoustic pulse without contributing to the environmental noise, and (c) the maximum usable frequencies at which the echo



sounder can operate as a function of meteorological conditions and range.

It was found that:

1. A ninety degree side lobe attenuation factor relative to the main beam of -97 dB will prevent the environmental ambient noise from seriously impairing the echo sounder sensitivity in the most noisy urban commercial environment.

2. Distances required to separate the acoustic antenna and the nearest potential listener, so that the transmitted signal cannot be heard, range up to 1500 meters in the most quiet, rural localities. However, when factors peculiar to a specific site are considered, these isolation radii can be reduced to reasonable distances in most cases.

3. An operational frequency of 8.0 kHz can be used for low altitude sensing or to several hundred meters. For higher altitude sensing of one kilometer or more, 2 kHz will be the maximum usable frequency for wide ranges of atmospheric humidity and temperature.

Phase II of this report describes (1) the design philosophy and mode of operation of the Wave Propagation Laboratory (WPL) Mark II Echo Sounder, and (2) the results of experiments with echo sounding equipment to determine (a) sidelobe radiation annoyance levels, (b) ratios of echo signal to ambient noise obtainable with a directional antenna, and (c) improvements in (a) and (b) achieved by placing anechoic shielding around the antenna.

The work reported here is a direct follow-on to the construction and operation of the WPL Mark I Echo Sounder (Wescott, et al., 1970). The improved Mark II system is currently in the field, gathering further data on acoustic Doppler wind sensing, temperature inversion structure, and boundary layer convection dynamics.

This work was supported both by NOAA research funds and by the Environmental Protection Agency.



## 2. PHASE I - SYSTEM ANALYSIS OF THE OPERATION OF ACOUSTIC SOUNDERS

### 2.1 Environmental Noise Levels

Environmental noise levels may determine if it is feasible to operate the sounder. The environmental ambient noise data used for this study were obtained from noise surveys found in the literature. Table 1 lists the locations and conditions under which the surveys were taken, the location numbers that will be referenced in this report, and a reference to the publications from which the data were taken.

Although the surveys considered here were made in specific locations, they represent a rather complete cross-section of the types of populated areas into which the acoustic echo sounder might be placed. Consequently, the noise data taken from these surveys provide a representative basis for predicting the interaction of the echo sounder with its potential environment. The analysis results will be indicative of what can be expected in any future application.

The data published in each survey were in the form of sound pressure levels in dB (referred to the threshold of hearing or  $0.0002 \text{ dynes/cm}^2$ ) for octave bands of the audible spectrum, usually up to 10,000 Hz. Many of the surveys gave more than one sound pressure level in dB for each octave band. This spread of data is the result of statistical analyses, representing values above or below which a percentage of the levels in the octave band occurred. For the purposes of this study, only the minimum and maximum values given were used. The former were used in the study to determine the effect of the acoustic echo sounder on the inhabitants in the surrounding community and the latter were used for the study on the amount of environmental noise received by the acoustic echo sounder antenna. This purposefully conservative approach was used in order to provide a margin of safety against falsely optimistic conclusions on the feasibility of acoustic echo sounding in urban environments.



Table 1. Locations and Conditions Under Which Environmental Noise Data Were Recorded.

Number	Location	Conditions	Reference
2	Chicago, Ill. (1950)	Residential; minimum night	Bonvallet (1951)
6		Residential; and commercial areas with little or no traffic	
7		Residential; unidentifiable backgrounds	
14		Commercial areas; fast auto traffic, light truck and commercial traffic	
16	Coral Gables, Florida (1968)	Residential; industrial backgrounds	Blazier (1968)
18		Industrial area	
19		Commercial areas, busy downtown heavy traffic	
4		Residential; ambient, no air conditioners operating	
9	New Jersey (1963)	Residential; 15 feet from 11 window or wall air conditioners	Ostergaard & Donley (1964)
10		Residential; 15 feet from 28 central air conditioners	
13		Residential; 20 feet from 22 central and room air conditioners	
5		Residential; spring, 9:00-11:00 p.m., heavily wooded suburban and parks	
8	State College (1955)	Residential; late summer, one family houses, daytime	Bateman & Ackerman (1955)
12		Residential; late fall, duplex dwellings, daytime	
11		Campus, during class hours	
15		Commercial, noisy downtown sidewalk, 5:00 p.m.-12 midnight	
17	Rural area	Commercial, noisy downtown sidewalk, 8:00 a.m.-5:00 p.m.	Berendt et al. (1967)
3		Daytime-near highway	
1		Daytime-no highway noise	
20		Near large metropolitan airport	
21	Jet Aircraft Takeoff	One mile slant height both sides	
22		1500 feet slant height both sides	
23		2-3 miles in front	
24		200 feet in front	
25		200 feet in back	



## 2.2 Environmental Noise Received by the Acoustic Antenna

Environmental ambient noise can present a problem when the acoustic echo sounder is operated in or near populated areas. The spectrum of the noise covers a broad band of frequencies which include the possible operating frequencies of the echo sounder. If the noise levels are too high, weakly scattered acoustic echoes from the atmosphere could be masked. It was necessary to determine what noise levels could be expected at various possible locations of operation and how seriously the noise would affect the echo sounder.

The acoustic antenna is a directional device, but because of diffraction it has sensitivity in directions other than the main lobe. As a result, the amount of environmental noise received by the echo sounder will depend not only on the noise levels existing at the antenna, but on the antenna sensitivity in the direction of incidence. The evaluation that follows will present a relation between the environmental noise and the antenna side lobe suppression necessary for operating the acoustic echo sounder in the various environments.

Johnson noise or thermal noise generated in the transducer element of the acoustic antenna represents a practical minimum of background noise that can be realized by the acoustic sounder (Nyquist, 1928). This limiting level of noise provides the basis to which the environmental noise is referred, determining the signal to noise ratios. We define an ambient noise figure,  $F$ , as the ratio of environmental to Johnson noise powers,

$$F = 20 \log \frac{V_a(\nu, \theta)}{V_j} . \quad (1)$$

Here  $V_a(\nu, \theta)$  is the rms voltage developed at the acoustic sounder transducer terminals by the spectral component,  $\nu$ , of the noise incident on the antenna from the direction  $\theta$ , and  $V_j$  is the thermal or Johnson noise voltage developed at the same terminals. The ambient noise figure,  $F$ , relates the environmental noise spectrum levels incident on the antenna to the side



lobe suppression required for satisfactory performance. Consequently when the signal-to-Johnson noise ratio is known, the amount of side lobe suppression necessary for successful operation can be determined for each possible environment.

When the explicit expressions for  $V_a(\nu, \theta)$  and  $V_j$  are substituted into (1) (as shown in Appendix A), the noise figure can be written as

$$F - 20 \log \epsilon(\nu, \theta) = 137 + SL_a + 20 \log \alpha(\nu) - 10 \log T \quad (2)$$

We define the quantity on the left of (2) as the noise suppression figure. The second term on the left is the antenna side lobe attenuation factor relative to the main beam in decibels and it is determined experimentally as discussed elsewhere in this report. The value to be used will be determined by the direction of incidence of the noise on the antenna. Here  $SL_a$  is the sound pressure spectrum level (or noise level per hertz) in decibels of the incident environmental noise,  $T$  is the absolute temperature of the atmosphere, and  $\alpha(\nu)$  is the antenna-transducer efficiency expressed in millivolts per dyne per square centimeter.

A nomograph of (2) is shown in figure 1 for an atmospheric temperature of  $20^\circ\text{C}$ . Since the acoustic antenna-transducer efficiency, as well as  $SL_a$  and  $20 \log \epsilon(\nu, \theta)$  are functions of frequency, the nomograph provides a convenient means of determining the various parameters at any frequency. For example, suppose the measured  $\alpha$  at 2000 hertz is 25 millivolts per dyne per square centimeter. What is the required side lobe suppression ( $90^\circ$  from the main lobe) at this frequency to give a noise figure of 15 dB when the sound pressure spectrum level of the environmental noise incident on the acoustic antenna ( $90^\circ$  from the main lobe) is 11 dB? The dashed lines indicate a side lobe suppression of -76 dB at 2000 Hz is required. Under these conditions the received environmental noise would be 15 dB above the Johnson noise; the signal-to-Johnson noise ratio would have to be at least this value to allow effective operation of the echo sounder.



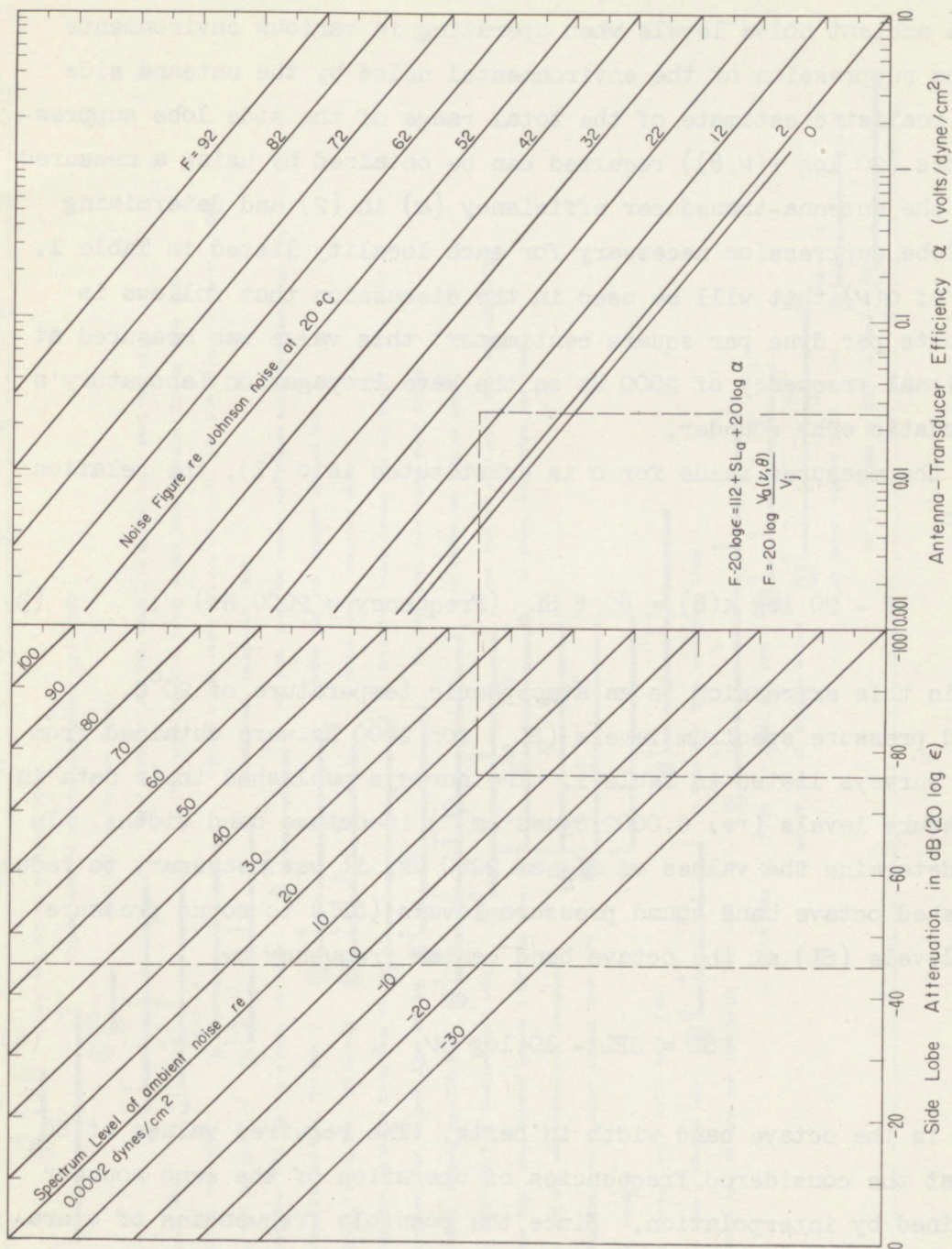


Figure 1. A nomograph relating the antenna-transducer efficiency ( $\alpha$ ), the ambient noise figure ( $F$ ), the acoustic antenna side lobe attenuation ( $20 \log \epsilon$ ), and the sound pressure spectrum level ( $SL_a$ ) of the environmental ambient noise. The assumed temperature is 20°C.



The important characteristic of the echo sounder that will determine acceptable ambient noise levels when operating in various environments will be the suppression of the environmental noise by the antenna side lobes. A realistic estimate of the total range of the side lobe suppression factors ( $20 \log \epsilon(\nu, \theta)$ ) required can be obtained by using a measured value for the antenna-transducer efficiency ( $\alpha$ ) in (2) and determining the side lobe suppression necessary for each locality listed in Table 1. The value of  $\alpha(\nu)$  that will be used in the discussion that follows is 25 millivolts per dyne per square centimeter; this value was measured at an operational frequency of 2000 Hz on the Wave Propagation Laboratory's Mark I acoustic echo sounder.

When the measured value for  $\alpha$  is substituted into (1), the relation reduces to

$$F - 20 \log \epsilon(\theta) = 80 + SL_a \text{ (Frequency = 2000 Hz)} . \quad (3)$$

Implicit in this expression is an atmospheric temperature of  $20^\circ\text{C}$ .

Sound pressure spectrum levels ( $SL_a$ ) for 2000 Hz were obtained from the noise surveys listed in Table 1. The surveys published their data in sound pressure levels (re.  $0.0002 \text{ dynes cm}^{-2}$ ) in octave band widths. In order to determine the values of  $SL_a$  at 2000 Hz, it was necessary to reduce the published octave band sound pressure levels (SPL) to sound pressure spectrum levels (SL) at the octave band center frequency by

$$SL = SPL - 10 \log \Delta\nu_a , \quad (4)$$

where  $\Delta\nu_a$  is the octave band width in hertz. The required values of  $SL_a$  existing at the considered frequencies of operation of the echo sounder were obtained by interpolation. Since the possible frequencies of operation being considered are 1, 2, 3, 4, and 5 kHz, the reducing-interpolation procedure was carried out for each frequency for the sake of future reference and the results are shown in figure 2.



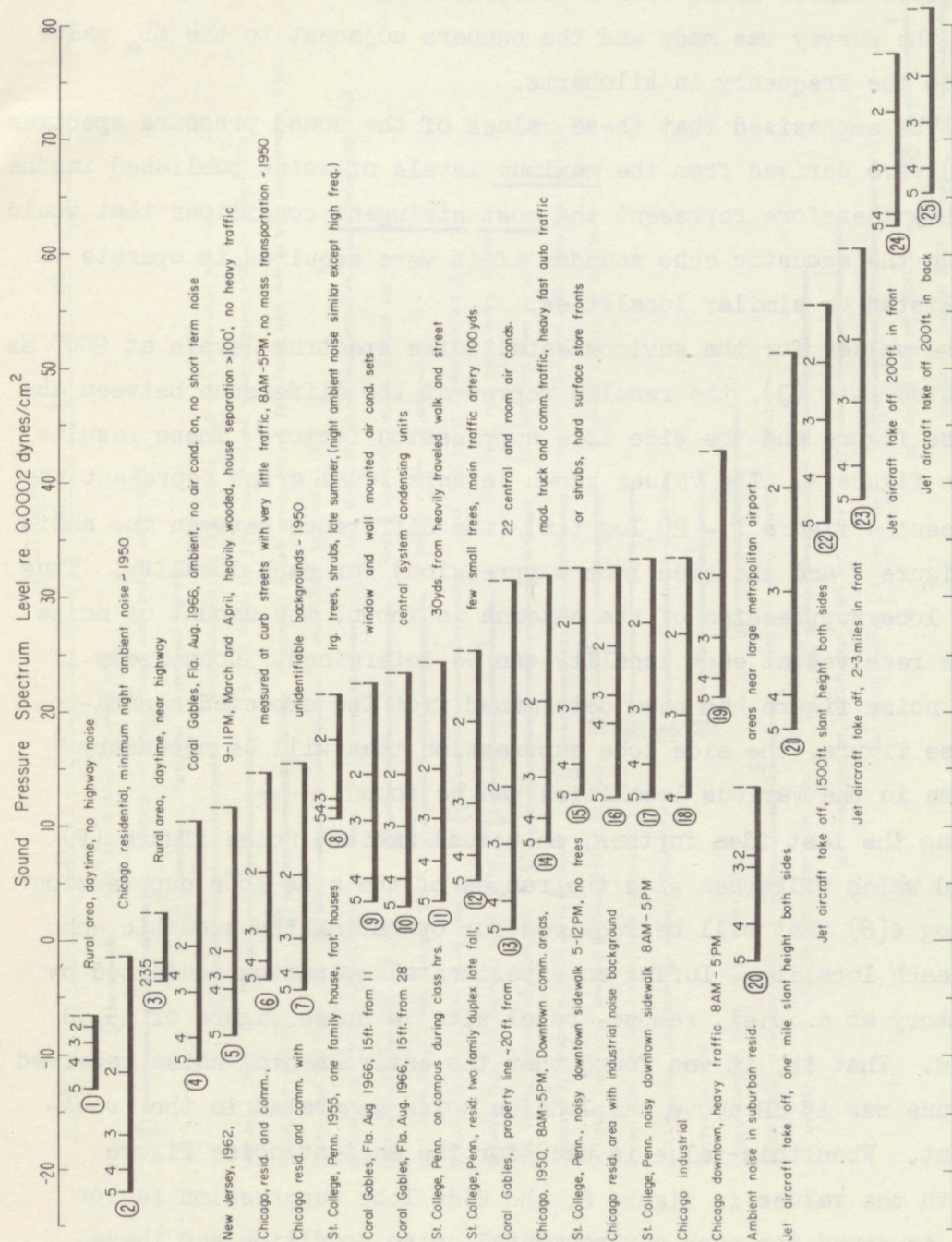


Figure 2. A level bar graph of the ambient noise sound pressure spectrum levels at 1, 2, 3, 4, and 5 kHz for the environments considered. The levels were calculated from data furnished in the references cited in table 1 and, where possible, maximum noise levels were used.



The localities listed in Table 1 have been arranged in Fig. 2 by ascending order of  $SL_a$  at 1000 Hz. Each locality is identified with a circled location number along with a brief description of the conditions under which the survey was made and the numbers adjacent to the  $SL_a$  value bars refer to the frequency in kilohertz.

It must be emphasized that these values of the sound pressure spectrum levels ( $SL_a$ ) were derived from the maximum levels of noise published in the surveys. They therefore represent the most stringent conditions that would be imposed on the acoustic echo sounder if it were required to operate in any of the listed or similar localities.

When the values for the environmental noise spectrum levels at 2000 Hz are substituted into (3), the results represent the difference between the ambient noise figure and the side lobe suppression factor. These results are shown in figure 3. The values shown in this level graph represent the noise suppression figure  $F - 20 \log \epsilon(\theta)$  (the difference between the ambient noise figure  $F$  and the side lobe suppression) for each locality. Thus if the side lobe suppression of the antenna is known, the amount of noise that will be received at each locality can be determined. Conversely if the ambient noise figure has been determined from the expected signal-to-Johnson noise figure, the side lobe suppression that will be necessary for operation in the various localities can be found.

Pursuing the last idea further, an actual ambient noise figure ( $F$ ) will be used which will then give the ranges of the side lobe suppression factor  $20 \log \epsilon(\theta)$  that will be required for operating the acoustic echo sounder in each locality. During an experimental operation conducted by this laboratory at a quiet, remote, rural site, a noise figure of 15 dB was measured. That is, it was found that the environmental noise received by the antenna was 15 dB above the Johnson noise generated in the transducer element. When this value is used for the ambient noise figure together with the values in figure 2, the side lobe suppression factor  $20 \log \epsilon(\theta)$  is found for each environmental noise condition and these values are shown in figure 4 for the acoustic frequency of 2000 Hz.



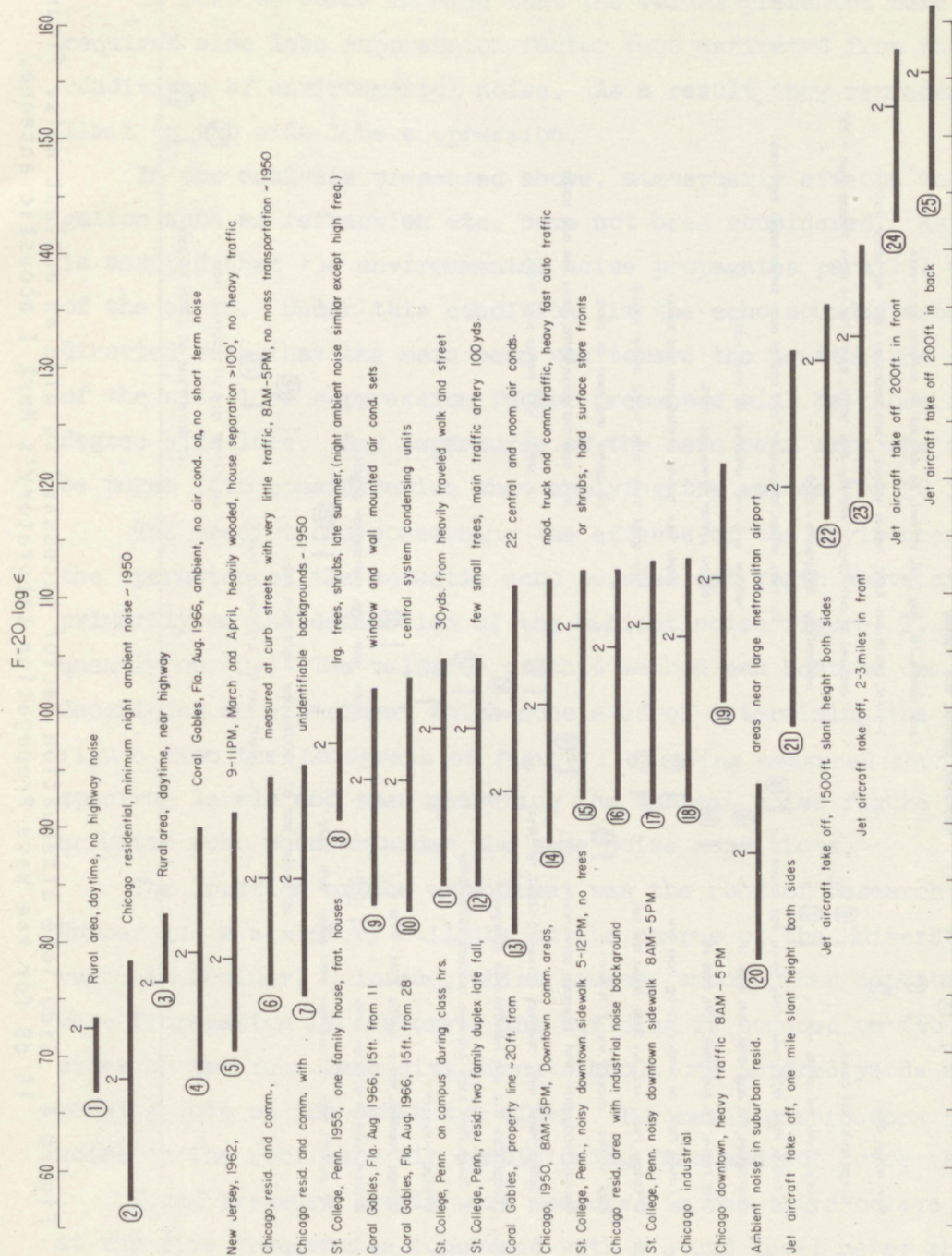


Figure 3. Noise suppression figure in dB between the ambient noise figure  $F$  and the side lobe attenuation factor  $20 \log \epsilon(\theta)$  for an antenna-transducer efficiency 0.025 volts/dyne/cm<sup>2</sup> at 2 kHz. The bar indicates the level difference range for the frequencies 1 to 5 kHz at the same  $\alpha(v)$ .



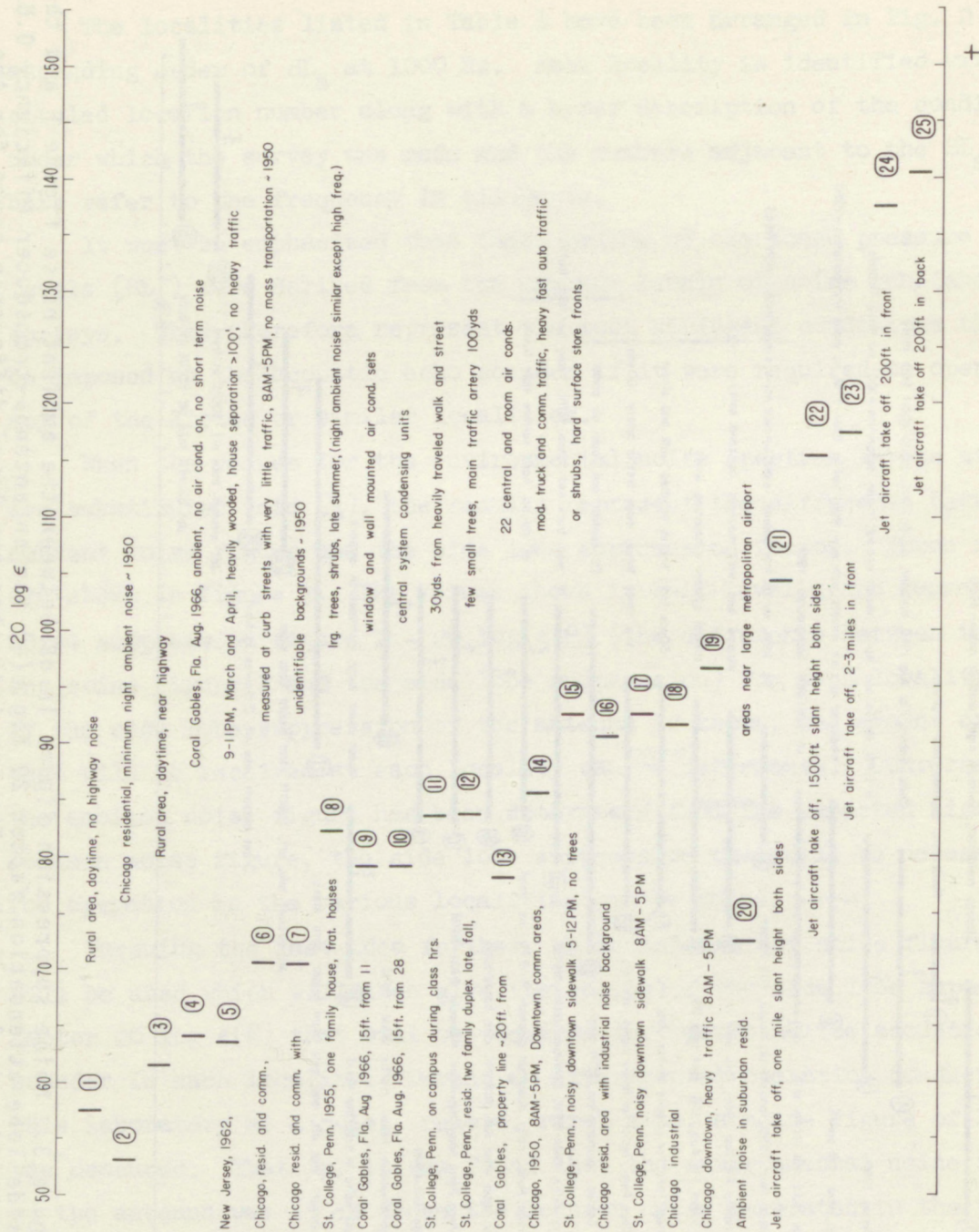


Figure 4. Side lobe attenuation factor necessary to give an ambient noise figure of 15 dB for the Wave Propagation Laboratory's Mark I acoustic antenna.



It must be borne in mind that the values presented here for the required side lobe suppression factor were estimated from the extreme conditions of environmental noise. As a result, they represent an upper limit on the side lobe suppression.

In the analysis presented above, atmospheric effects on sound propagation such as refraction etc. have not been considered. As a result, it is assumed that the environmental noise propagates parallel to the surface of the earth. Under this condition, if the echo sounder antenna were directed such that the main beam was toward the zenith, the values of the side lobe suppression factor presented will be those for the ninety degree side lobe. Any departures of the main beam from the zenith must be taken into consideration when applying the values for  $20 \log \epsilon(\theta)$ .

The predictions concerning the effects of the environmental noise on the operation of the acoustic echo sounder set forth above are based primarily on the definition of the ambient noise figure,  $F$ , and subsequently on (2). The validity of this method can best be demonstrated by describing an experiment which consisted of determining the ambient noise figure from the nomograph of figure 1 by using measured sound pressure spectrum levels and then measuring the ambient noise figure with the acoustic echo sounder under the same noise conditions.

The location of the experiment was the roof of Research Building Number 3: a six story building on the campus of the University of Colorado, in Boulder, Colorado, which houses, among other departments, the Wave Propagation Laboratory. The building is bounded on two adjacent sides by two four-lane city streets about one hundred yards away and parking lots on the other two sides. The main contributors to the noise on the roof were air conditioning fans and not motor vehicles.

Sound pressure levels were measured in one third octave band widths at the five frequencies concerned with a sound level meter and a calibrated omni-directional microphone. Sound pressure spectrum levels,  $SL_a$ , were determined from these measurements as described earlier and are listed in Table 2.



Table 2. Environmental Sound Pressure Spectrum Levels at RB-3,  
Boulder, Colorado

Frequency	SL <sub>a</sub> (dB)
1000 Hz	20
2000 Hz	11
3000 Hz	4
4000 Hz	-1
5000 Hz	-4

In order to determine the expected ambient noise figure for the acoustic echo sounder, the antenna-transducer efficiency and the antenna side lobe suppression factor must be known. For the echo sounder and a frequency of operation of 2000 Hz that was used, they are  $25 \times 10^{-3}$  volts/dyne/cm<sup>2</sup> and -45 dB respectively; the latter figure is for the ninety degree side lobe which applies when the main beam is directed toward the zenith.

Using these values for  $\alpha$ ,  $20 \log \epsilon(\theta)$ , and SL<sub>a</sub> (at 2000 Hz) in the nomograph, figure 1, it can be seen that the predicted ambient noise figure is 45 dB, i.e., the amount of environmental noise received by the echo sounder would be 45 dB above the Johnson noise generated in the transducer coil.

The actual ambient noise figure was measured by placing the acoustic antenna at the same position on the roof that the sound level microphone occupied for the sound level measurements. A resume of these results is presented in Table 3 and it is seen that the measured noise figure of 43 dB above the Johnson noise is in good agreement with the value predicted from noise level measurements.

The agreement of these two results serves to demonstrate the validity of the method for determining the expected ambient noise figure. Thus in future applications, when a particular location is being considered as a possible place of operating the acoustic echo sounder, the noise figure can be predicted merely by measuring the sound pressure level at the site and making use of the nomograph in figure 1.



*Table 3. Acoustic Background Noise Measured at 2000 Hertz with a Fiber Glass Parabolic Horn Antenna With the Main Beam Vertical.*

Noise signal input to wave analyser receiver  $V_o = 2.5 \times 10^{-3}$  volts rms.

System voltage gains

Input transformer	32 dB
Preamp gain	24 dB
Interstage transformer	15 dB
TOTAL	71 dB

Noise signal voltage at the transducer-terminals

$$V_N = V_o - (71 \text{ dB gain}) = 7.0 \times 10^{-7} \text{ volts rms}$$

Thermal noise voltage at the transducer terminals

$$V_j = 4kTB = 5.1 \times 10^{-9} \text{ volts rms } 20^\circ\text{C}$$

Ambient noise figure

$$F = 20 \log \frac{V_N}{V_j} = 43 \text{ dB}$$



### 2.3 The Effects of Acoustic Power Radiated in Side Lobes

Excessive sound radiated in the side lobes of the acoustic antenna will present a problem when operating the acoustic antenna in populated areas. If the level of this side lobe sound field is high enough, the echo sounder could represent a noticeable source of irritating noise. Utilizing the echo sounder in connection with air pollution meteorology could result in the instrument itself contributing excessively to noise pollution. This situation would be intolerable. A study was therefore made to determine the conditions necessary for operating the echo sounder such that the side lobe radiation would produce acceptable levels of sound.

The study involved looking for a means by which the psychological effects induced by sound stimuli could be predicted when a physical description of the sound is known. Four methods were studied and considered for the problem, two of which were found to be applicable and two of which were not. Of the two schemes used, the more basic one makes use of the masking effect of pure tones by noise. The second one, used as a check, deals with predicting the reaction of a community from a physical description of the sound stimuli. The two methods that were considered, but not used here were schemes by which the subjective aspects of "loudness" (Stevens, 1961) and "noisiness" (Kryter and Pearsons, 1963) of the audible stimuli could be predicted from a physical description of the sound. These two schemes were not used because they required a decision to be made as to what will be considered too "loud" or too "noisy".

The masking effect of noise was used as the basis for determining the operating conditions. Fletcher's hypothesis (1940) is that a small "critical" bandwidth of white noise can mask a pure tone that is presented in the noise. Fletcher suggested that the masking bandwidth of the noise is such that the acoustical power in the band is just equal to the power of the pure tone if the band of noise is centered on the frequency of the pure tone. This hypothesis thus sets a criterion for operating the echo sounder so that the inhabitants in the area surrounding the antenna cannot hear it.



A determination of the effective masking present involves finding the sound pressure levels in the environmental noise for each frequency of operation considered and for each of the typical environments listed in Table 1. These masking levels in turn will determine the maximum sound pressure levels in the side lobe sound field that can exist in the surrounding community and not be heard. By using these maximum levels and the known side lobe radiation characteristics, an isolation radius for the antenna can be found by assuming the antenna to be a point source.

A method due to French and Steinberg (1947) based on Fletcher's criterion was used to calculate the maximum side lobe sound pressure levels that are just masked by the environmental noise. For this method, the effective masking level  $z(\nu)$  of the environmental noise is given by

$$z(\nu) = \left[ SL_a + K(\nu) \right] - \beta_o(\nu) \quad (5)$$

This equation represents the amount by which the level of the noise in the critical bandwidth exceeds the level of the minimum audible field (MAF) of a pure tone. The sound pressure spectrum level of the environmental noise is  $SL_a$ , and the sound pressure level of the MAF in dB above  $0.0002 \text{ dynes/cm}^2$  is  $\beta_o(\nu)$  and  $K(\nu)$  is the critical bandwidth of the noise in dB referred to one hertz. The values for  $K(\nu)$  and  $\beta_o(\nu)$  have been determined experimentally (French and Steinberg, 1947; Hawkins and Stevens, 1950; Robinson and Dadson, 1957) and they are given in Table 4 for the frequencies concerned here.



Table 4. Octave-band and Critical-band Conversions and Binaural Minimum Audible Field Levels.

fc	$\Delta\nu_a$	Conversion to Spectrum Level	Critical Band Width	$\Delta\nu_c$	Binaural MAF $\beta_o$
		$10 \log_{10} \Delta\nu_a$	$K \approx 10 \log_{10} \Delta\nu_c$		re 0.0002 dynes/cm <sup>2</sup>
Hz	Hz	dB	dB	Hz	dB
1000	707	28.5	16.2	42	4
2000	1414	31.5	18.5	71	1
3000	2121	33.3	20.0	100	-3
4000	2828	34.5	21.1	129	-4
5000	3535	35.5	21.9	155	1

The values for  $SL_a$  were determined from the surveys listed in Table 1 by the same procedure discussed in the preceding section and they are shown in figure 5. By using these values in (5), the effective masking level was calculated for each frequency and location considered.

Each calculated value of  $z(\nu)$  was then used to find the corresponding value of the masking level  $M(\nu)$  by using the empirical relation shown in figure 6 after Hawkins and Stevens (1950). (This was a necessary step because the two quantities are not always equal as shown in the figure.) Finally the masked threshold ( $\beta(\nu)$ ) was calculated by the relation

$$\beta(\nu) = M + \beta_o(\nu) , \quad (6)$$

and the results are shown in figure 7. The bars shown in the figure for each of the five operational frequencies (1, 2, 3, 4, and 5 kHz) correspond to the values of masked threshold values in dB (re 0.0002 dynes/cm<sup>2</sup>) and the circled numbers refer to the location numbers in Table 1.



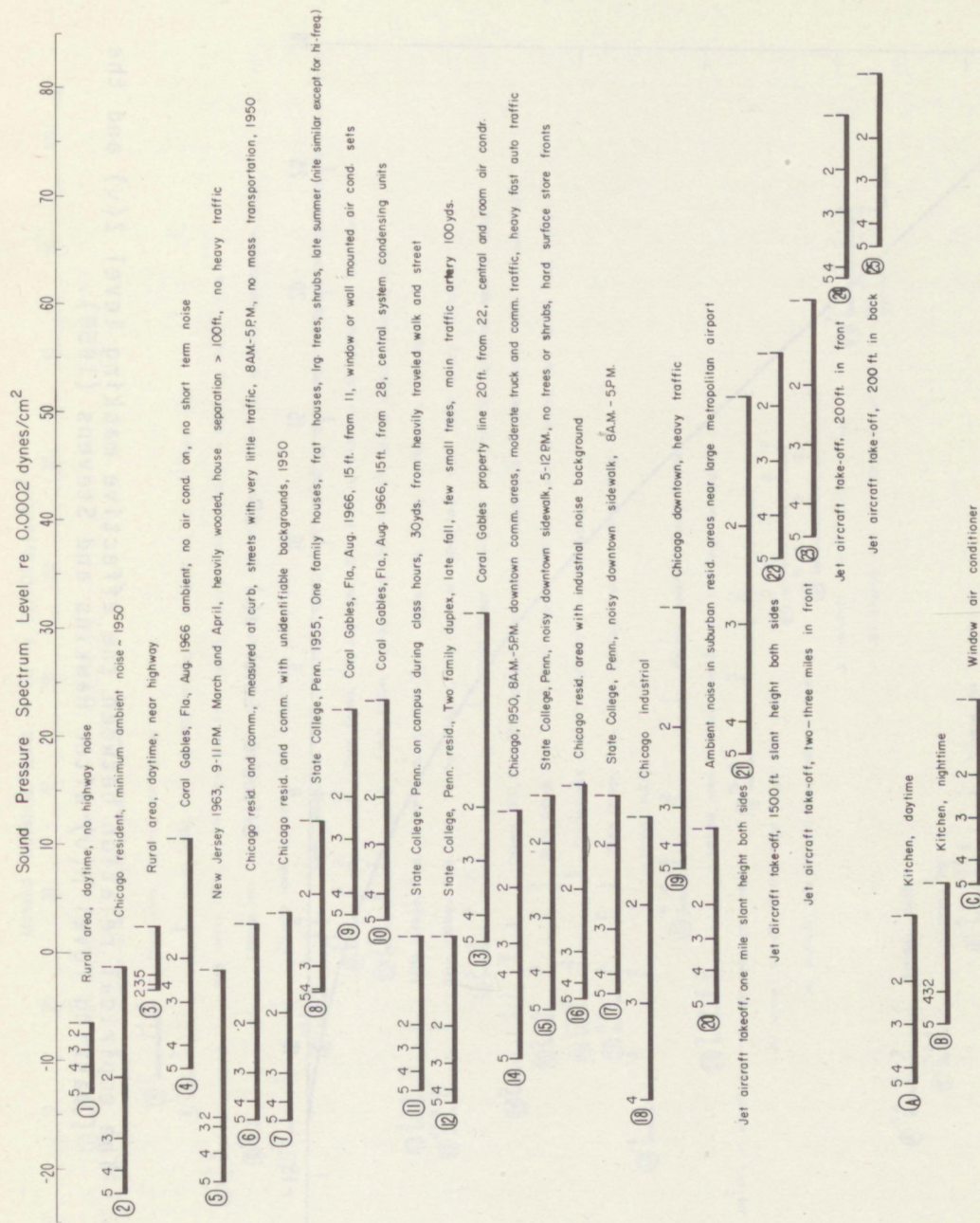


Figure 5. A level bar graph of the ambient noise sound pressure spectrum levels at 1, 2, 3, 4, and 5 kHz for the environment considered. The levels were calculated from data given in the references in table 1 and, where possible, minimum noise levels were used.



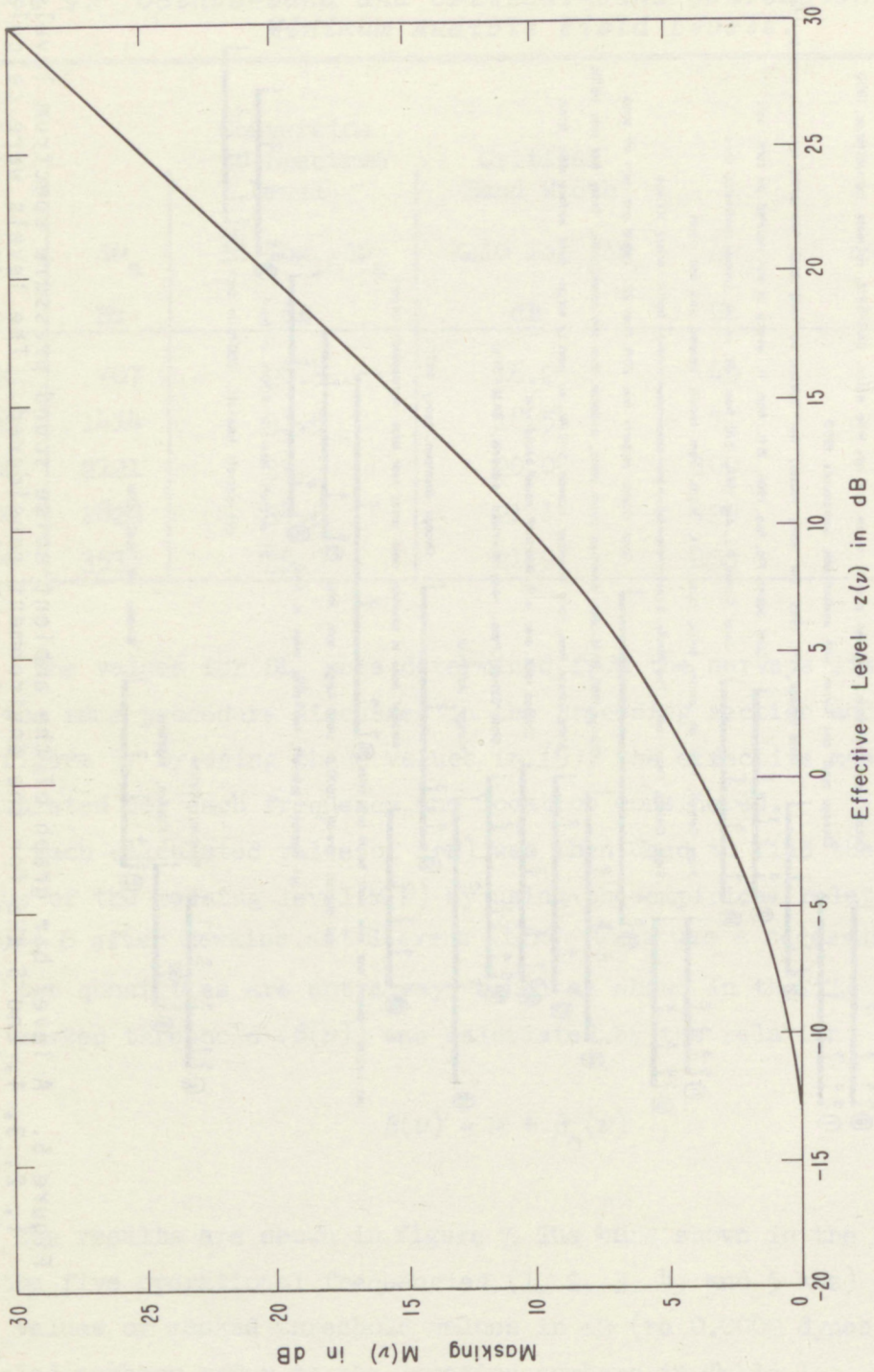


Figure 6. The empirical relation between the effective masking level  $Z(\nu)$  and the masking level  $\beta(\nu)$  after Hawkins and Stevens (1950).



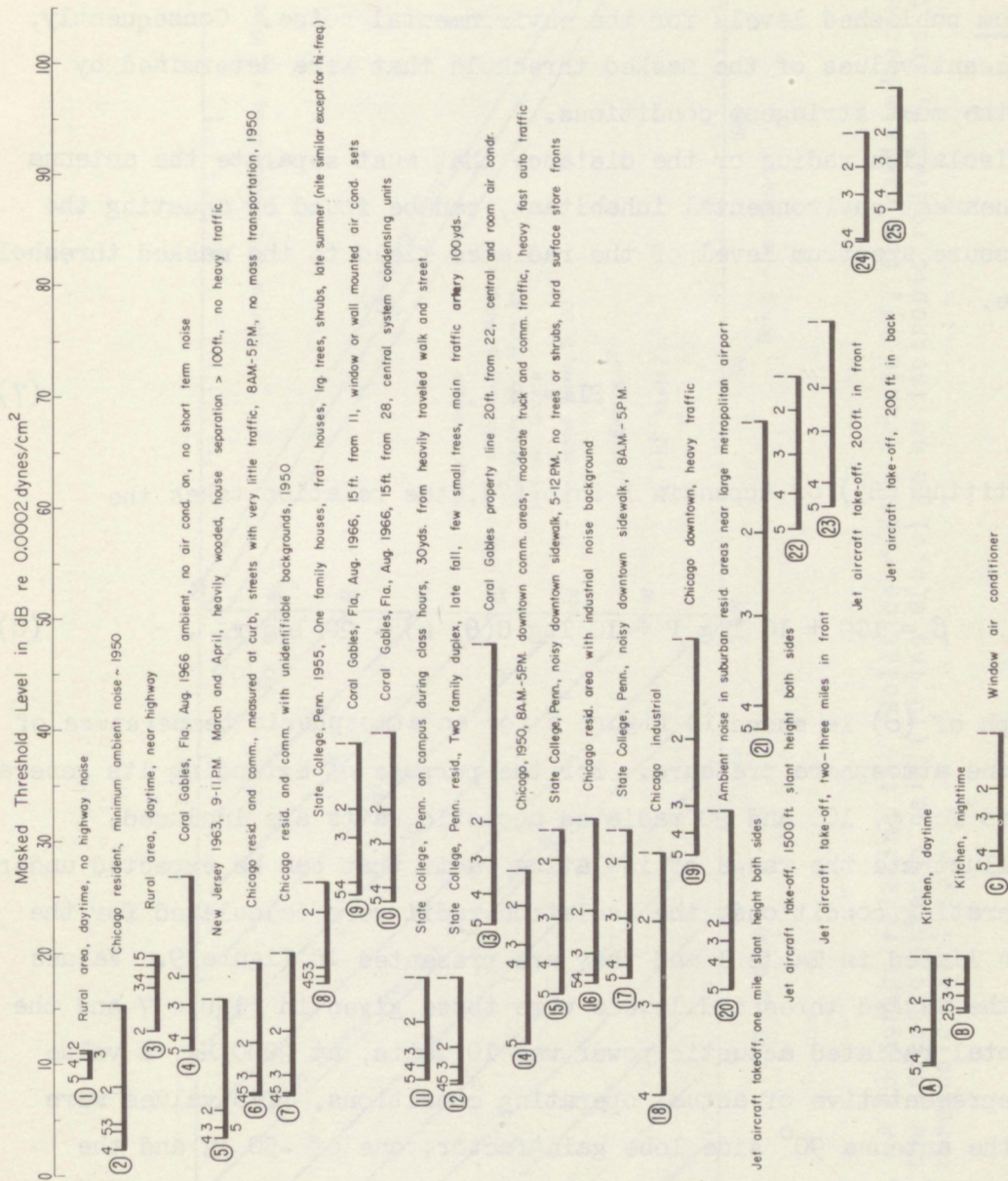


Figure 7. A level bar graph of the masked threshold level  $\beta(v)$  for the frequencies 1, 2, 3, 4, and 5 kHz. These represent the level of a pure tone in dB (re 0.0002 dynes/cm<sup>2</sup>) that will be just masked by the environmental ambient noise.



These values of the masked threshold represent the sound pressure spectrum levels of the sound radiated in the antenna side lobes that can be just masked by the environmental noise. They were calculated by using the minimum published levels for the environmental noise. Consequently, they represent values of the masked threshold that were determined by imposing the most stringent conditions.

The isolation radius or the distance that must separate the antenna from its nearest environmental inhabitant, can be found by equating the sound pressure spectrum level of the radiated field to the masked threshold level, i.e.

$$SL = \beta \quad . \quad (7)$$

By substituting (B5) of Appendix B into (7), the relation takes the form

$$\beta = 109 + 10 \log P + 10 \log G(\theta, \nu) - 20 \log r \quad . \quad (8)$$

A nomograph of (8) is shown in figure 8 for an atmospheric temperature of 20°C and one atmosphere pressure. For the purpose of extending its general use, curves for 5, 10, and 20 radiated acoustic watts are included.

To illustrate the range of isolation radii that can be expected under actual operating conditions, the isolation radii were calculated for the localities listed in Table 1 and they are presented in figure 9. Values used for the masked threshold levels were those given in figure 7 and the assumed total radiated acoustic power was 10 watts, at 2000 Hz, a value that is representative of actual operating conditions. Two values were used for the antenna 90° side lobe gain factor; one of -50 dB and the other -60 dB as indicated by the wedge and circle respectively. The two values used for the antenna side lobe gain factor (relative to an isotropic radiator) are representative of values measured on the ninety degree side lobe of the acoustic antenna at 2000 hertz. Details of the measurements are given in Section 3.1 of this report. Without the hay bale acoustic



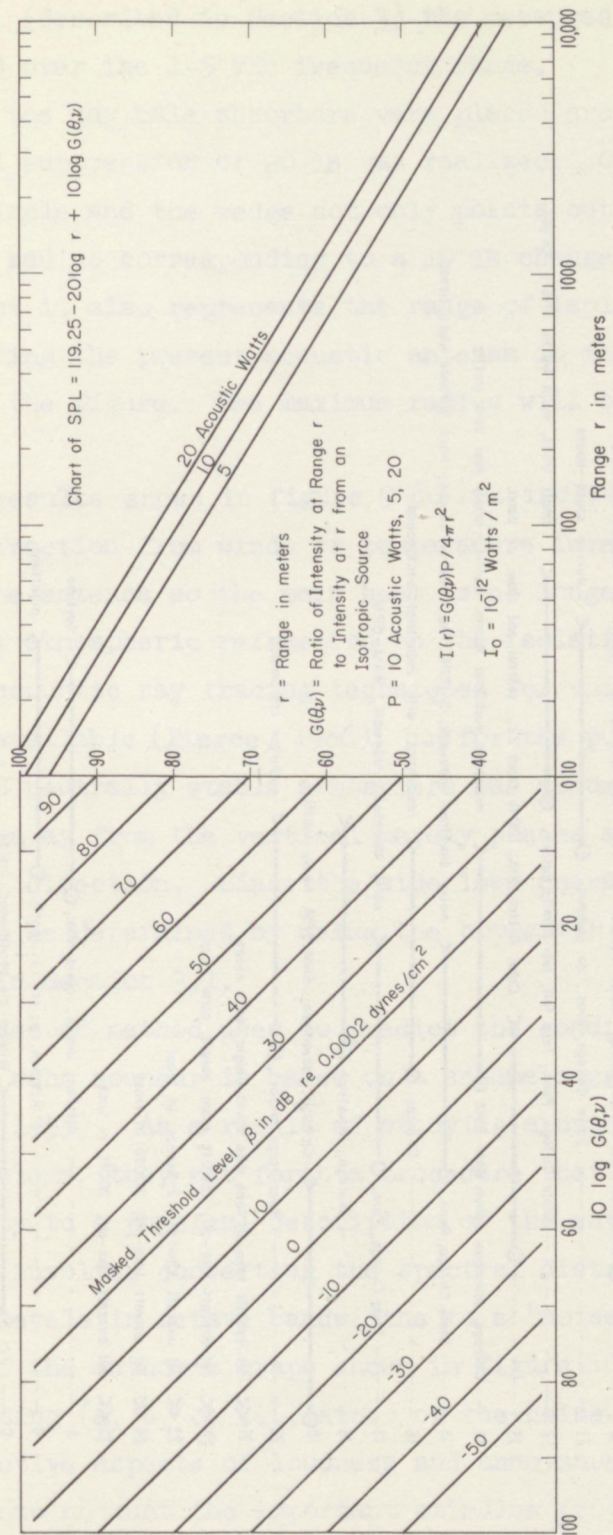


Figure 8. A nomograph relating the isolation radius (range  $r$ ), the radiated acoustic power, the acoustic antenna gain ( $10 \log G(\theta, \nu)$ ) re an isotropic radiator, and the masked threshold level  $\beta$ .



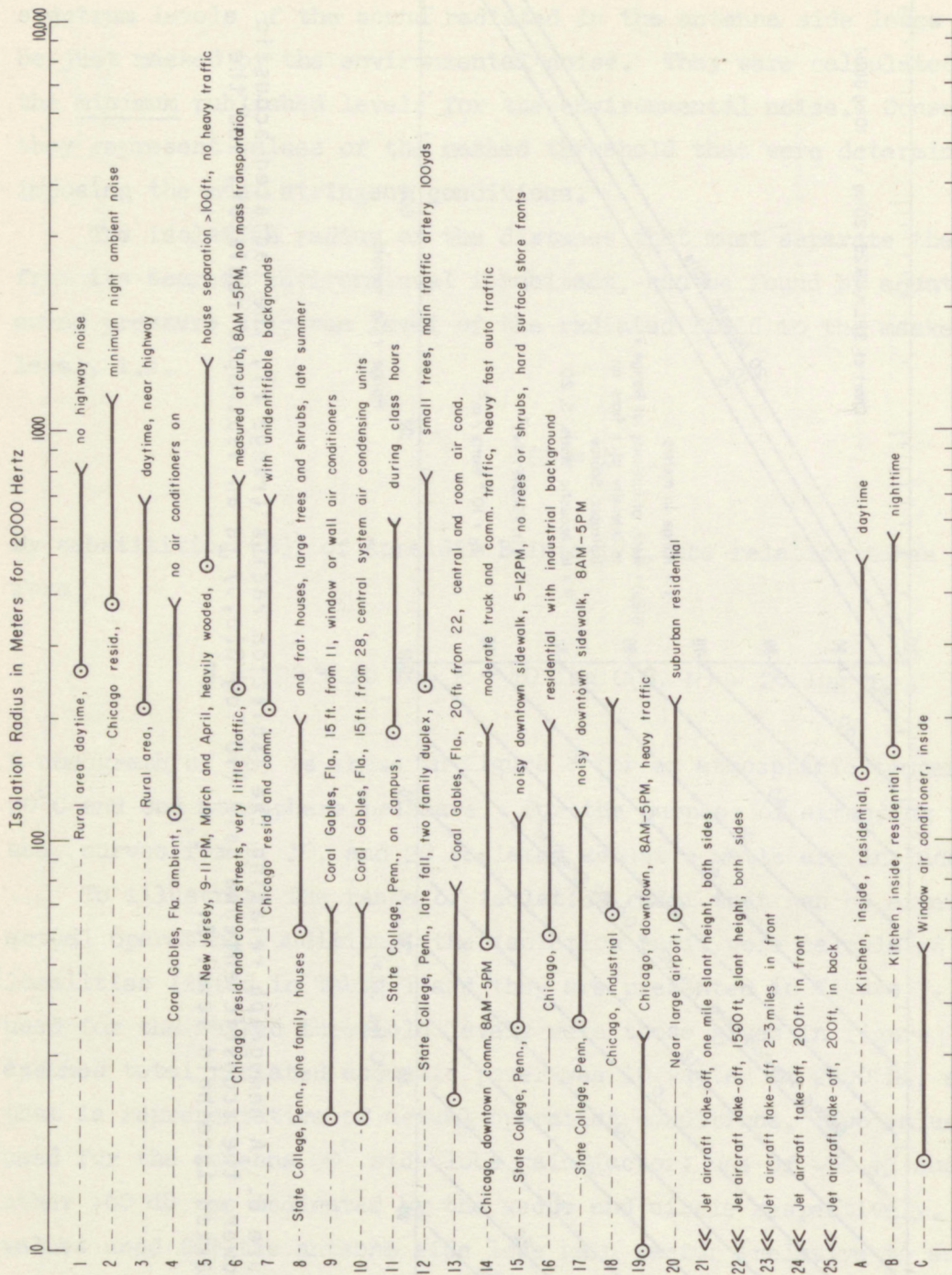


Figure 9. The acoustic antenna isolation radii for the environments considered. These are the distances that must separate the acoustic antenna and the nearest potential listener so that the echo sounder cannot be heard. The wedge and circle are for an antenna gain factor  $[10 \log G(90^\circ, 2000 \text{ Hz})]$  of -50 dB and -60 dB (re an isotropic radiator) respectively.



shielding, (described in Section 3) the measured value was between -30 and -35 dB over the 1-5 kHz frequency range.

When the hay bale absorbers were placed around the antenna, a minimum additional suppression of 20 dB was realized. Consequently, the line joining the circle and the wedge not only points out the reduction in the isolation radius corresponding to a 10 dB change in the antenna gain factor, but it also represents the range of isolation radii to be expected for operating the present acoustic antenna in the typical locations represented in the figure. The maximum radius will be that indicated by the wedge.

The results shown in figure 9 do not include the effects of atmospheric refraction from winds or temperature inversions, or the effect of tilting the antenna so the main beam is no longer along the vertical. Effects of atmospheric refraction on the isolation radius can be estimated by using acoustic ray tracing techniques for which there are computer programs available (Pierce, 1966), but for the purposes of this report a static and neutrally stable atmosphere was assumed. Tilting the antenna main beam away from the vertical merely places another side lobe along the horizontal direction. Since the side lobe characteristics are known, this effect can be determined by using the nomograph of figure 8 and beam patterns reported in Section 3.1.

The second method used to predict the conditions necessary for operating the echo sounder is based on a scheme suggested by Stevens, Rosenblith, and Bolt (1955). As a result of studying a number of case histories of noise problems, they set forth a procedure that relates the reactions of a community to a physical description of the environmental noise. The procedure involves converting the spectral distribution of the noise sound pressure levels in octave bandwidths to a "noise level rank" (nlr) with the aid of the author's graph shown in figure 10. This is a lower case letter rating (a, b, c, ..., etc.) of the noise that takes into account the subjective aspects of loudness and annoyance. The nlr is then adjusted to take into account the important stimulus properties that affect a communities' reactions. The result is the "composite noise rating", (CNR),



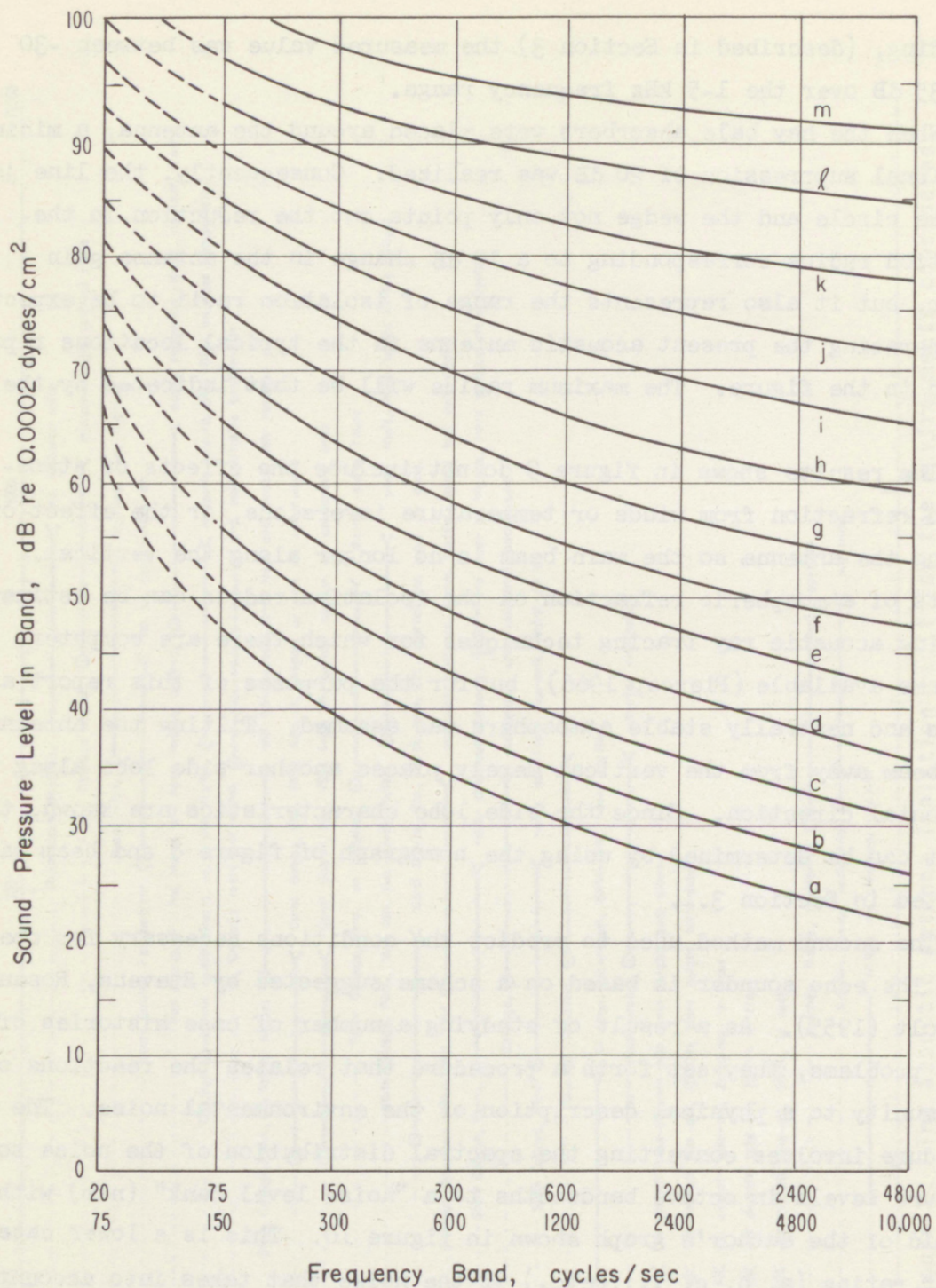


Figure 10. Family of curves used to convert the noise level rank to sound pressure levels for 1, 2, 3, 4, and 5 kHz (after K. N. Stevens et al., 1955).



in capital letters. Finally, the predicted response of the community can be found from a graph similar to the one shown in figure 11.

For the present problem, the suggested procedure was reversed. A CNR was chosen that, on the average, corresponded to a communities' response of "no observed reaction." The CNR was then converted to a physical description of the noise (in this case the antenna side lobe sound field) that could exist without invoking any community response. The results are shown in Table 5 for an operational frequency of 2000 hertz.

Figure 10 was used to obtain sound pressure levels (re 0.0002 dynes/cm<sup>2</sup>) in column four of Table 5 from the noise level ranks in column three. Octave band sound pressure levels were reduced to spectrum levels at the octave band center frequencies by the usual method, and the spectrum levels for 2000 hertz were found by interpolation. The spectrum levels for the letter ranks a-, a=, and a≡ were determined by extrapolating the family of curves in the figure to one, two, and three letter changes. Octave band sound pressure levels for the center frequency of 2000 Hertz were found by adding  $10 \log \Delta \nu_0 = 32$  dB to each spectrum level.

The sound pressure levels listed in column four for each environment represent the maximum permissible levels of the sound field in the side lobe radiation that can exist and still provoke "no observed reaction" by the communities. These levels are to be compared with those listed in figure 7. Although the environments listed in figure 7 are specific localities, they do correspond to the more general listing in Table 5. example, location number 1 of figure 7 would correspond to a "Very Quiet Suburb (night)" environment in Table 5.



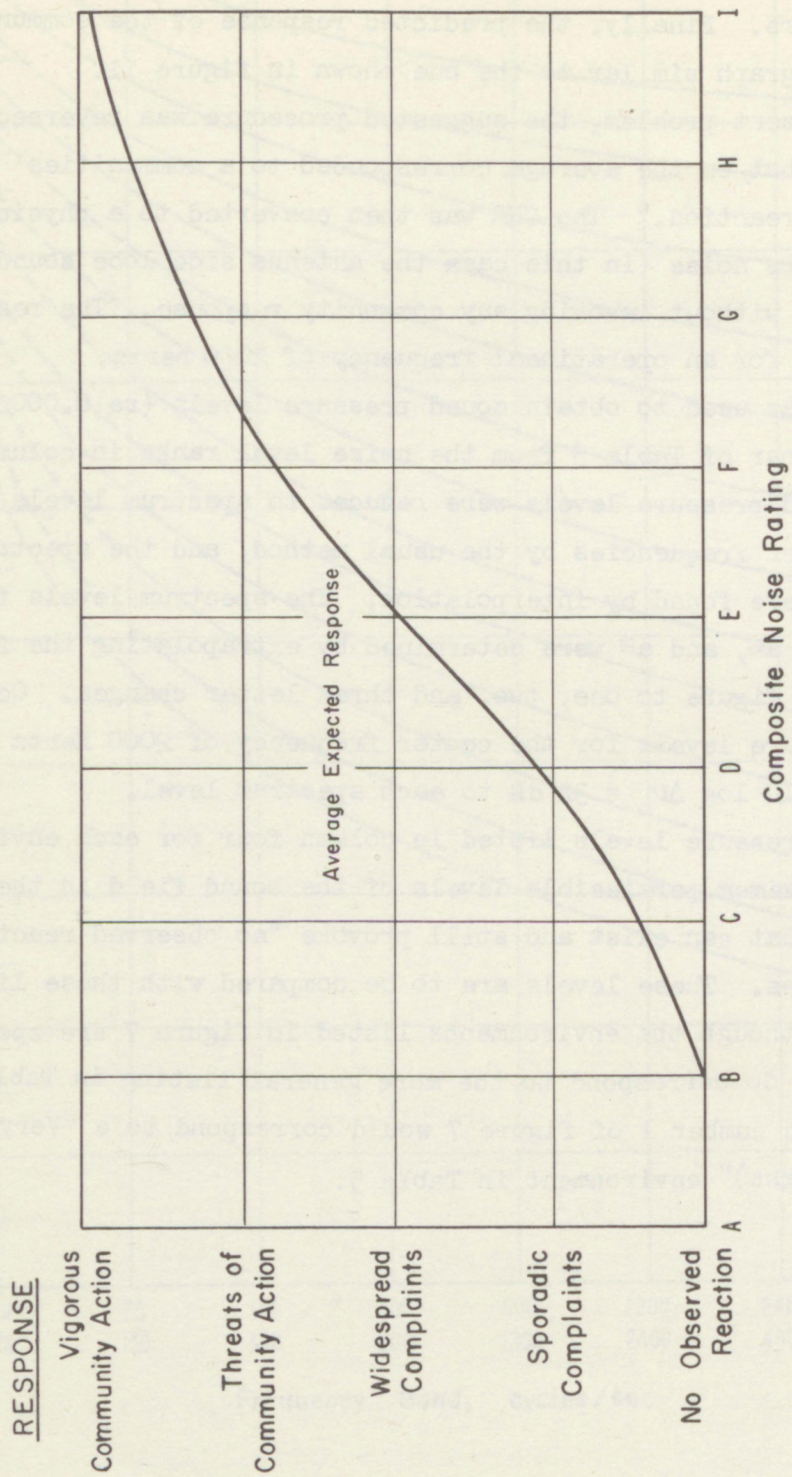


Figure 11. Community "Response" versus Composite Noise Rating after K. N. Stevens et al. (1955).



Table 5. Calculation of Maximum Antenna 90° Side Lobe Radiation at 2000 Hz From the Predicted Response of the Community.

I. Maximum Response: "No Observed Reaction"

Composite Noise Rating: B

II. Adjustment for Effective Stimulus Characteristics

Composite Noise Rating	B
Previous Exposure	0
Peak Factor	-1
Spectrum Character	-1
Winter or Summer	0
Repetitive Character	0
Day or Night	0
<hr/>	
Intermediate Noise Level Rank	(a-)

III. Adjustment for Background Noise.

Environment	Adjust.	Noise Level Rank (nlr)	SPL (dB) 2000 Hz
Very Quite Suburb (night)	-2	a≡	12
" " " (day)	-1	a=	16
Suburban (night)	-1	a=	16
" (day)	0	a-	21
Residential Urban (night)	0	a-	21
" " (day)	+1	a	26
Urban Near Industry (night)	+1	a	26
" " " (day)	+2	b	30
Heavy Industry (night)	+2	b	30
" " (day)	+3	c	34



In comparing these maximum permissible sound levels, it will be seen that there is a fair agreement between the results of the two methods except that the latter "community" results are more tolerant of noise by four or more decibels. This is a result of imposing the most severe conditions for the "masking" method, i.e., the lowest levels of ambient environmental noise were used. If the nominal levels had been used, this discrepancy would be reduced. Using the sound levels in Table 5 to calculate isolation, the radii shown in figure 9 would be reduced by approximately 1/1.7.

In the preceding paragraphs, two methods were used to calculate the maximum acceptable sound pressure levels that can exist in the antenna side lobe field for various environments. The agreement between the results of the two methods gives confidence that they represent, with adequate accuracy, the permissible side lobe fields. The resulting isolation radii listed in figure 9 represent the maximum distances required to separate the acoustic antenna and the nearest potential listener for each of the typical localities. However, when a specific site is chosen for operating the acoustic echo sounder, factors peculiar to the site may tend to reduce the actual operating isolation radius as discussed in Conclusions, Section 4.



## 2.4 An Estimate of Useable Acoustic Frequencies

Sound waves propagating through the earth's atmosphere are attenuated by various mechanisms. The amount of attenuation depends on the path length, the meteorological conditions existing along the path, and the frequency of the sound waves. Because of the frequency dependence, it was necessary to determine the range of useable frequencies for operating the echo sounder as a function of meteorological conditions and range. The approach used was to relate the received echo signal level to attenuation coefficient and the range. Then by assuming a reasonable signal level, the maximum average attenuation coefficient as a function of range was determined which, in turn, specified the frequency range as a function of meteorological conditions.

The acoustic power received by the antenna from a scattering region at range,  $R$ , made up of diffuse scatterers with an average cross-section per unit volume of  $\sigma$  is given by the acoustic radar equation

$$P_r = \frac{P_o}{R^2} \frac{c\tau}{2} \sigma (A_r \eta) \exp(-2 \int_0^R \kappa(R) dR') \quad (9)$$

where  $P_o$  is the transmitted acoustic power,  $c$  is the speed of sound,  $\tau$  is the transmitted pulse length,  $(A_r \eta)$  is the effective antenna cross-section (on axis), and the exponential describes the amount of attenuation suffered by the transmitted pulse in traveling the round trip. The effective acoustic intensity of the received echo is

$$I_r = \frac{P_r}{A_r \eta} = \frac{P_o}{R^2} \frac{c\tau}{2} \sigma \exp(-2 \int_0^R \kappa(R) dR') \quad (10)$$



which is related to the acoustic pressure amplitude,  $p$ , of the received echo by

$$p = \sqrt{\rho c I_r} \quad (11)$$

where  $(\rho c)$  is the acoustic impedance of the air at the antenna aperture,  $\rho$  is the air density and  $c$  is the velocity of sound. The open circuit rms voltage,  $v_r$ , developed at the transducer terminals is obtained by multiplying (11) by  $\alpha$  the antenna transducer efficiency.

$$v_r = \alpha \sqrt{\rho c I_r} \quad (12)$$

The signal level,  $S$ , in dB above the Johnson noise voltage for a 1 Hz bandwidth is

$$S = 20 \log \frac{v_r}{v_j} = 20 \log \frac{v_r}{\sqrt{4kT\Omega}} \quad , \quad (13)$$

where  $T$  and  $\Omega$  are, respectively, the absolute temperature and resistance of the transducer element and  $k$  is Boltzmann's constant. Substituting (10) and (12) in (13) and assuming:  $T = 293^\circ\text{K}$ ,  $\rho c = 415 \text{ kg m}^{-2} \text{ sec}^{-1}$ ,  $\Omega = 16 \text{ ohms}$ ,  $P_o = 10 \text{ acoustic watts}$ ,  $\sigma = 7.2 \times 10^{-3} \text{ C}_T^2 \text{ T}^{-2} \tau^{-1/3}$  and  $C_T = 4.64 \times 10^{-2} \text{ deg} \cdot \text{m}^{-1/3}$ , the equation for the signal level takes the form

$$S = 154.82 + 10 \log \tau - \frac{10}{3} \log f - 20 \log R - 8.68 \int_0^R \kappa(R) dR' \quad . \quad (14)$$

In order to evaluate (14), we would have to know  $\kappa$  for each point along the path of propagation which, in turn, would require a knowledge of the meteorological conditions existing along the path. It would be impractical at this point to consider all of the possible combinations of meteorological parameters, therefore an average attenuation coefficient,  $\bar{\kappa}$ , may be written as



$$\bar{\kappa} = \frac{1}{R} \left( 14.58 + 1.152 \log \tau + 0.384 \log f - 2.303 \log R - \frac{S}{8.68} \right) . \quad (15)$$

The third term involving the frequency dependence occurs as a result of the  $\lambda^{-1/3}$  dependence of the scattering cross section per unit volume,  $\sigma$ .

By assuming a reasonable signal to Johnson noise level of say 20 dB, we find that (15) will give the maximum allowable average attenuation coefficient as a function of range with the pulse duration as a parameter. The variation of  $\bar{\kappa}$  with frequency (for the range 1000 to 6000 hertz) is small at the higher ranges and for the present purpose a frequency of 3000 hertz was used.

Before the maximum attenuation coefficients obtained from (15) can be used to determine the usable acoustic frequencies, it was necessary to investigate the meteorological phenomena that contributed to the attenuation of sound waves in air.

The attenuation coefficient can be divided into three parts:

$$\kappa = \kappa_c + \kappa_m + \kappa_e . \quad (16)$$

These are called, respectively, the classical, molecular, and excess attenuation coefficients. Classical attenuation is the result of sound absorption due to the effects of viscosity, heat conduction and radiation, and molecular diffusion. The behavior of this term is well known (Sivian 1947) and it is generally considered to be small compared to the other two for the frequencies considered here. Molecular attenuation is concerned with the absorption of sound due to a relaxation process involving a lag in the adjustment of the vibrational energy of  $O_2$  molecules during the passage of the sound wave. The term,  $\kappa_e$ , takes into consideration the losses due to refraction and beam bending resulting from temperature and wind velocity gradients, inertial and thermal scattering caused by turbulent wind and temperature fluctuations, and miscellaneous absorption.



Of the two terms,  $\kappa_m$  and  $\kappa_e$ , that contribute the most to the attenuation coefficient,  $\kappa_m$  is the one about which the most is known. The effects of molecular absorption have been measured in the laboratory by Evans and Bazley (1954), Harris (1963, 1966), Harris and Tempest (1964), and Henderson, Clark and Lintz (1965).

It is difficult at this time to include in this report the effects of the third term in (16), i.e. attenuation of sound due to other mechanisms such as refraction, scattering, etc. At present there has not been sufficient theoretical or experimental work performed to allow an adequate explanation to be formulated about the behavior of this phenomenon. It is a source of attenuation that must be considered not only for the present purposes but also in analysing data recorded by the echo sounder. For these reasons, there is an urgent need for further work to be done in an attempt to understand this attenuation mechanism. Delsasso and Leonard (1953) found that the laboratory measured values of the attenuation coefficient were less than those values measured under atmospheric conditions. They attributed the excess attenuation in the open air to refraction and turbulence effects. Beran, et al., (1970) have measured the excess attenuation coefficient for sound in the real atmosphere and found it to vary from a negligible correction to twice the value given by the molecular attenuation effect. For the purpose of this report, however, the excess attenuation coefficient was not included because of the lack of definitive information.

Harris (1966) presents a graph of the molecular absorption coefficient versus relative humidity with frequency of sound as a parameter. These are laboratory data measured at 20°C and atmospheric pressure. A portion of this graph is shown in the upper left of figure 12. From (15) a maximum average attenuation coefficient can be found for a given  $\tau$ ,  $S$ ,  $f$ , and  $R$ . Using the resulting  $\bar{\kappa}$  on Harris's graph allows the combination of the average relative humidity and frequency to be determined. It was convenient to extend this idea by combining a graph of (15) with Harris's data and this is given in figure 12. The graph of (15) represents the maximum



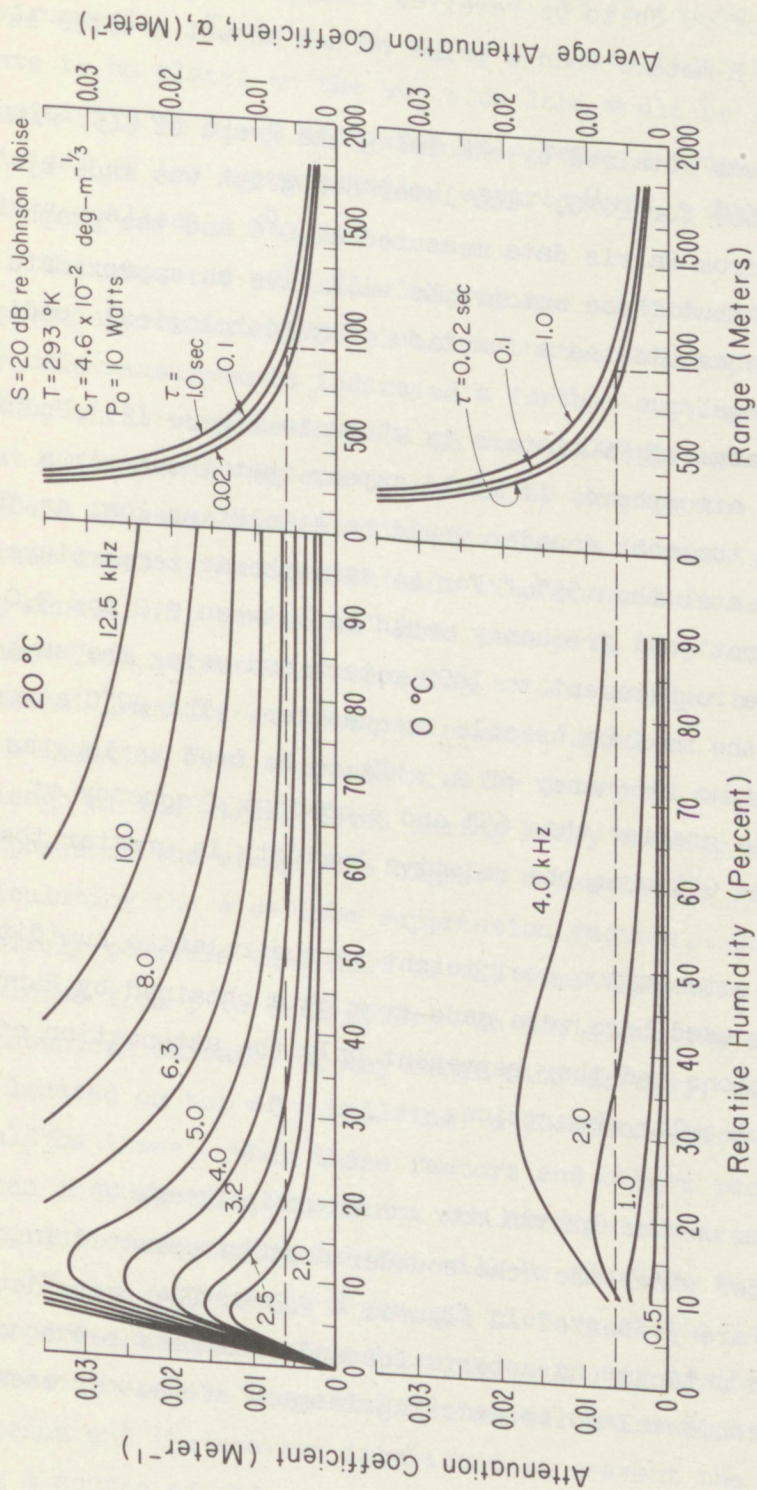


Figure 12. Nomographs for determining the range of operating frequencies for an acoustic echo sounder.



average attenuation coefficient (the ordinate  $\bar{K}$ ) that will allow a signal-to-Johnson noise level of 20 db to be received from a scattering region at the range (abscissa) R meters when a pulse of ten acoustic watts is transmitted.

The top nomograph was obtained by combining the graph of (15) with one given by Harris (1966) for 20°C. The lower nomograph was made by combining a graph made from Harris data measured at 0°C and the graph of (15). It is intended that these nomographs will give an approximate range of operational frequencies as a function of meteorological conditions (humidity) and range.

An example for a range of 900 meters is shown in figure 12. Under the condition of a 20°C atmosphere, it would appear that the maximum frequency for operating the echo sounder would be 4.0 kHz as long as the relative humidity is greater than 55%. For an atmospheric temperature of 0°C, the maximum operational frequency would be between 2.0 and 3.0 kHz.

Extending the range requirement to 1800 meters and using the same  $\tau = 0.1$  sec, decreases the maximum useable frequencies. The 20°C atmosphere would allow a maximum frequency of 2.5 kHz to be used as long as the relative humidity is greater than 65% and a maximum frequency of approximately 1.5 kHz at 0°C when the relative humidity is greater than approximately 45%.

The curves of the attenuation coefficient versus relative humidity at the two temperatures used here, were made from data obtained by Harris under laboratory conditions and they represent only the attenuation of sound resulting from molecular absorption.

## 2.5 Conclusions on the Operability of Acoustic Sounders

The conditions under which the echo sounder must be operated in populated environments are presented in figures 4 and 9. They were determined from the measured antenna characteristics and from measured sound level data of the environmental noise existing in each of the representative localities.



In figure 4 it is seen that the required side lobe attenuation factor of the acoustic antenna ranges from -53 dB to -97 dB for non-aircraft environments. That is, according to these figures, the extreme requirements to be placed on the  $90^{\circ}$  side lobe would be that its receiving sensitivity be 97 dB below the main beam in order to operate in the noisiest of the representative environments. The question arises: is this a realizable figure?

The measured  $90^{\circ}$  side lobe of the antenna without acoustic shielding was approximately 50 dB below that of the main beam. Results of the hay bale measurements indicated a further suppression by a minimum of 20 dB, which results in a 70 dB overall suppression. It is expected that a further 20 dB can be gained by shaping the aperture illumination to be a Gaussian spatial distribution in intensity and constructing a better acoustic antenna shield. The end result should be that the receiving sensitivity of the  $90^{\circ}$  side lobe will be 90 dB below that of the main beam. This represents according to the results a 7 dB deficit for the noisiest location at location number "19".

Location "19" represents noise data that were recorded in downtown Chicago at the street level during heavy traffic conditions. For the purposes of the study, the highest noise levels reported were used in calculating the side lobe suppression factors. Consequently, it is entirely possible that most of the time the noise levels at the location could be from 5 to 8 dB lower. In addition, the echo sounder, if located in downtown Chicago, or any other similar city, would more than likely be located on top of a building; a location where the street noise levels would be lower. When these factors and others peculiar to the site are taken into account, it is not too difficult to realize side lobe suppression requirements that will be adequate for this location.

Figure 9 presents a general picture of the isolation radii required to operate the acoustic echo sounder in any of the representative environments. These are suggested distances that must separate the acoustic antenna and the nearest inhabitant to prevent the echo sounder from becoming a source of objectionable noise. They range from 34 meters to 1500



meters and the question arises is it possible to satisfy these distance requirements in any specific environment. To answer this question, it will be necessary to consider not only the conditions used to calculate these radii but also other existing factors that were not used and to what extent they will influence the results.

It will be remembered that these radii were (indicated by the wedge) calculated from an antenna gain factor of  $10 \log G (90^\circ, 2000 \text{ Hz}) = -50 \text{ dB}$  and the levels of noise required to mask a pure tone were determined from the minimum (where possible) ambient environmental noise levels. Therefore, these distances should represent the maximum expected radii and any reduction will be the result of adjusting the antenna gain factor and/or the masking level.

The antenna gain factor can be improved in two ways. Results of the hay bale acoustic shield experiment suggest that a well constructed acoustic shield will decrease the amount of sound radiated in the ninety degree side lobes. Also, calculations made on the antenna aperture diffraction pattern indicate that a significant decrease in side lobe radiation can be expected when the aperture is illuminated with a plane acoustic wave whose pressure distribution is an axially symmetric Gaussian. It is expected that these two improvements will result in at least a 15 dB to 20 dB improvement in the antenna gain factor at ninety degrees.

Other factors that will decrease the isolation radii requirements are associated with the masking effect of the environmental noise. These factors will be acoustical conditions that are peculiar to a specific site and although it is difficult to assess all of them here a few will be considered to demonstrate their effects.

Psychoacoustically, a pure tone stimulates a different sensation of loudness than a pulsed tone. Munson (1947) has shown that a pulsed tone whose duration is less than approximately 250 millisecc does not appear as loud as a cw tone. Garner (1947) has demonstrated that a pulsed 2000 Hz tone whose duration was 20 millisecc can have a sound pressure level



approximately 5 dB above a cw tone of the same frequency and still be masked by the same noise level. This phenomenon will effectively increase the masked threshold; the amount of increase will depend upon the duration of the pulse transmitted by the echo sounder.

A conservative estimate of a 5 dB increase in the masking level would be realized if the average ambient environmental noise levels were used instead of the minimum levels.

The presence of air conditioners and the structural conditions of houses will also affect the masking levels. For out-of-doors conditions, the effects of air conditioners can be seen by comparing location 4 to locations 9 and 10 in figure 9. In this location, the air conditioners raise the masking level approximately 15 dB. And the effect of a window air conditioner inside is illustrated by location C. Consequently, an increase of 5 dB to 10 dB in the masking level could be expected in most environments under summer time conditions. During the winter, the inhabitants of most localities would be indoors with their houses sealed against the weather. The attenuation of sound by the walls and windows of the houses would effectively increase the masking level 5 to 10 dB. Then for summer and winter time conditions an estimated 5 to 10 dB increase could be expected in the masking level.

The total effect of the factors considered above is a conservative increase of 30 dB in (8) which will reduce the isolation radii by approximately  $1/30$ . Applying this factor for example to location 5 of figure 9, the resulting isolation radius requirement is reduced to 50 meters, a figure that is more reasonable for this type of locality.

Whether these and other factors associated with a particular locality will be effective or not will depend on the specific site chosen for operating the echo sounder. However, the acoustic shield and the Gaussian aperture illumination alone will reduce the radii shown in figure 9 (indicated by the wedge) by at least a factor of  $1/5$ .



The operational frequencies for echo sounding in the atmosphere given in figure 12 were determined by assuming values of the parameters for the echo sounder and the atmosphere. Of the parameters and values assumed, two are questionable; the value of  $C_T$  may be too large, also molecular absorption may not be the only significant sound attenuation mechanism present in the atmosphere.

As for the assumed value of  $C_T$ , preliminary data analysis performed in this laboratory indicate that the assumed value of  $C_T$  is in the measured range. However, a value of  $C_T$  one order of magnitude smaller would decrease the average attenuation coefficient by an amount  $2.3/R$  which would give a maximum operating frequency of approximately 2500 Hz for a range  $R = 900$  meters. The nomograph then does allow a rough estimate to be made of the maximum operating frequencies if molecular absorption is the only attenuation mechanism present.

It is concluded that the Phase I study has shown that acoustic echo sounders can be operated at or near the acoustic transducer self-noise level in rural, urban, or industrial environments without being affected by the ambient noise levels. Sounders may be so designed and located in rural and urban areas so as not to produce unwanted noise pollution for the inhabitants. Atmospheric attenuation of sound will not limit useful ranges of atmospheric probing if the sounder is operated in the frequency range 1 - 2 kHz. Acoustic sounders constitute a valid tool for air quality control investigations. Acoustic sounder records of atmospheric returns should be obtained over an extended period of field operations, in all seasons, and under a variety of meteorological conditions to determine the value of an operational sounder system for routine air quality control work.

### 3. PHASE II - ECHO SOUNDER DESIGN AND EXPERIMENTAL RESULTS

Phase II of this report describes (1) the design philosophy and mode of operation of the WPL Mark II Echo Sounder, and (2) the results of experiments with echo sounding equipment to determine (a) sidelobe



radiation annoyance levels, (b) ratios of echo signal to ambient noise obtainable with a directional antenna, and (c) improvements in (a) and (b) achieved by placing anechoic shielding around the antenna. Additional results incidental to the above are also presented.

### 3.1 WPL MARK II ECHO SOUNDER

The Mark II Echo Sounder is a second generation system embodying many worthwhile engineering improvements while carrying on the general design philosophy of the Mark I sounder. Thus the new system continues to employ all solid-state electronics, utilizes a single antenna and transducer for both transmitting and receiving, and performs all transmit-receive switching operations without the use of mechanical relays. The elimination of mechanical relays is felt to be of paramount importance since, by virtue of switching with diodes and other solid-state devices, there has never been a shutdown of the Mark I or Mark II echo sounder due to faulty contacts or switching failures of any kind. A policy of building as much of the system as possible with laboratory-quality, commercially-available electronic instruments has been followed because of the flexibility, precision and dependability inherent in these instruments, and because a substantial amount of project time and manpower usually can be saved by buying factory-assembled equipment whenever feasible in preference to having such items constructed by project personnel. In line with this policy, even when an electronic instrument was not commercially available to serve as a complete system component, the component was built up from factory-assembled, solid-state, temperature-compensated, encapsulated amplifiers, power supplies, integrators, electronic switches, multipliers, etc. in order to minimize hand wiring, circuit debugging and maintenance problems, and to increase the calibration accuracy and stability of the finished component over a wide range of environmental field conditions.

The operation of the Mark II Echo Sounder can be followed from the block diagram of figure 13. Two sections of the system shown in figure 13 are still under construction, i.e. (1) the digital recording section which will contain a high-speed, multi-channel scanner or data sampler, an analog-to-digital converter and a digital tape recorder, and (2) the



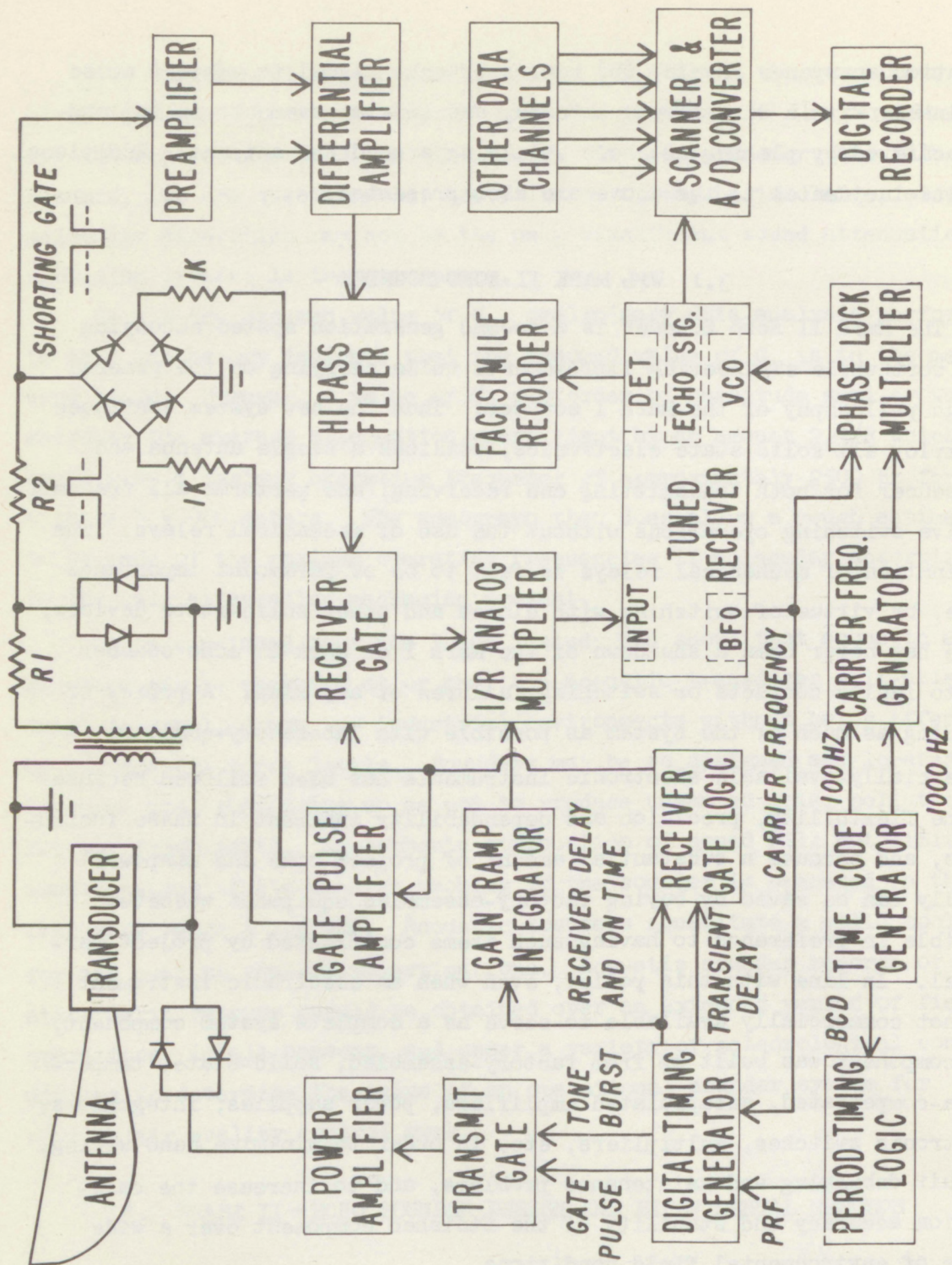


Figure 13. Block Diagram, Mark II Echo Sounder.



carrier frequency generator and phase-lock section which will lock the tuning of the narrow-band receiver and its BFO (beat frequency oscillator) to any choice of a number of highly stable carrier frequencies derived from the crystal-controlled oscillator of a time code generator. All other components of the Mark II system have been completed and are operational. Pending completion of the phase-lock section, the carrier frequency of the sounder is presently determined by adjusting the continuously variable BFO of the narrow-band receiver. The receiver is so constructed that the center of its pass band automatically coincides with the BFO frequency even as this frequency, not being crystal controlled, drifts slightly with temperature and line voltage variations.

The Mark II system differs from the Mark I primarily in that all timing functions are regulated by a crystal stabilized clock or time code generator. The future lock-in of carrier frequencies and receiver tuning has already been described. The block diagram of figure 13 also shows that the period timing logic of the system is controlled by a BCD (binary coded decimal) train of pulses from the time code generator. Period timing logic consists of a configuration of diode gates which pass a pulse only when the particular combination of zero and plus BCD levels occurs that corresponds to a desired PRF (pulse repetition frequency). Timing logic gates are currently provided for selecting PRF's of 0.5, 0.2 and 0.1 Hz (i.e. periods of 2, 5, and 10 seconds corresponding respectively to maximum echo ranges of about 1100, 2650 and 5500 feet).

The PRF signal is used to trigger a digital timing generator which in turn passes a tone burst of carrier frequency from the receiver BFO, generates a gate pulse coincident with the tone burst, and generates two additional pulses having start and stop times that may be delayed independently by desired amounts from the start of the tone burst. The duration of the tone burst and associated gate pulse, and the start and stop times of the other pulses are set to desired millisecond readings by means of digital thumbwheel switches on the timing generator. Tone burst durations ranging from 10 milliseconds to 1 second are normally used with the Mark II sounder depending upon whether maximum resolution, maximum range, or a compromise between resolution and range of echoes is desired.



As figure 13 shows, the tone burst from the timing generator is gated a second time as it passes through a transmit gate on the way to the transmitting power amplifier. The transmit gate is an FET solid-state switch with ON and OFF modes controlled by the gate pulse from the timing generator. The need for redundant gating of the tone burst became apparent when it was realized that the digital timing generator was providing only 60 dB of carrier frequency attenuation between gate pulses. The resulting carrier leakthrough was enough to create a very low level "false echo" signal during the echo sounder receive mode. The auxiliary transmit gate provides an additional 60 dB of carrier attenuation between gate pulses, and thus eliminates the carrier leakthrough problem.

The tone burst from the transmit gate is applied to the input of the power amplifier at a level of 1 volt rms. The gain of the power amplifier is adjusted to deliver 40 watts rms of electrical power through a pair of back-to-back diodes to a 16-ohm acoustic transducer for the duration of the tone burst. The transducer is coupled acoustically to a reflector-horn antenna. The overall transmitting efficiency of the transducer-antenna configuration is about 20%, so that the antenna radiates about 8 watts rms of acoustic energy into the atmosphere during the tone burst.

Between tone bursts, the power amplifier produces less than a millivolt of hum and instrument noise. This noise is none-the-less more than an order of magnitude larger than some of the extremely small voltages developed by the acoustic transducer in response to weak echoes. Back-to-back silicon diodes were therefore placed between the power amplifier and the acoustic transducer. These diodes readily conduct large-amplitude transmit tone bursts, but are virtual open circuits to signals of less than 300 millivolts rms. Power amplifier noise in the one-millivolt range is thus automatically isolated from the receive circuits of the echo sounder. In order for the diode isolation circuit to work reliably, however, it is essential that the power amplifier have a well regulated power supply. Otherwise power line surges will produce voltage fluctuations at the amplifier output large enough to pass through the diodes, and receiver overload will occur.



During transmission, it is necessary to isolate and protect the extremely sensitive receiver circuits of the echo sounder from overload and possible damage. This is done in three stages, and the circuit elements involved (mostly silicon diodes as shown in fig. 13) perform a task equivalent to that of a radar "T-R" device. The first stage is a set of back-to-back diodes in shunt with resistor R1. These diodes behave as the pair described above in that they are virtual open circuits to sub-millivolt echo signals, but low-impedance conductors to large-amplitude tone bursts. During transmission, therefore, almost all of the signal appearing at the secondary of the receive-circuit input transformer drops across R1. A clipped signal of about 1 volt P-P, determined by the conduction threshold potential of the diodes, remains at the junction of R1 and R2 during the transmit tone burst, but this residual signal is dropped across R2 by a second stage of receiver circuit protection.

The second stage is a diode bridge shorting gate. The action of this gate is controlled by the polarities of a pair of equal but opposite receiver gate pulses. When the polarities of these pulses are as shown in figure 13, all diodes of the bridge conduct, and the receiver preamplifier input terminal is thereby clamped to ground. When the polarities of the pulses are reversed, as they are throughout the receiver ON time, all diodes of the bridge are biased beyond cutoff, and the gate has no effect on the receiver circuit.

The pulses that control the action of the diode bridge shorting gate are obtained from the gate pulse amplifier. This block on figure 13 actually represents a pair of medium-current operational amplifiers (one inverting, the other non-inverting) to satisfy the 10 ma current requirement of the shorting gate. The gate pulse amplifier is driven by a composite pulse developed in the receiver gate logic section. The receiver gate logic is a form of AND gate which is activated by the combination of two different pulses from the digital timing generator, i.e. a Transient Delay pulse and a Receiver Delay/Receiver ON pulse. The start of the resultant pulse from the receiver gate logic is delayed from the beginning of the transmit tone burst by the number of milliseconds dialed into the Transient Delay thumbwheel switches of the digital



timing generator. Similarly, the stop time of the pulse is determined from the beginning of the tone burst by the sum of the Receiver Delay and Receiver ON dial settings. The start time of the pulse just described is chosen to delay the turn on of receiver circuits until the ringing or reverberation in the acoustic antenna caused by the powerful transmit tone burst has decayed to a negligible level. This is about 100 msec from the end of the tone burst for the fiberglass horn-reflector antenna now in use, and is equivalent to about the first 50 ft of echo range. It should be possible to reduce the reverberation time and subsequent loss of close-range echoes by future improvements in acoustic antenna design. The stop time of the pulse from the receiver gate logic is set to turn off the receiver circuits a few msec before the start of the next transmit tone burst. This is done as a precaution to protect the receiver circuits from possible damage by the initial transient of the transmit signal.

The relative timing of the tone burst and various pulses produced by the digital timing generator is illustrated by the waveform diagrams of figure 14. This figure also shows the resultant receiver gate pulse obtained by applying two different timing pulses to an AND gate in the receiver gate logic section. Finally figure 14 shows a gain ramp waveform used to provide receiver gain compensation for the spherical divergence or weakening of echo signals as they are received from progressively longer ranges. The start and reset times of this ramp are programmed to occur respectively at the center of the tone burst (by setting of Receiver Delay digital thumbwheels), and at the end of the Receiver ON time (as per sum of Receiver Delay and Receiver ON digital thumbwheel settings).

The gain ramp is started midway through the tone burst because of a decision to define zero echo range as occurring midway through the tone burst. This decision is based upon the distribution of echo signal strength from scattering volumes of finite thickness. For example, consider a scattering volume or layer in the atmosphere that has a thickness roughly the same as the spatial length of an acoustic tone burst that is about to propagate through the volume. Acoustic energy will be



## MARK II ECHO SOUNDER CONTROL SIGNALS

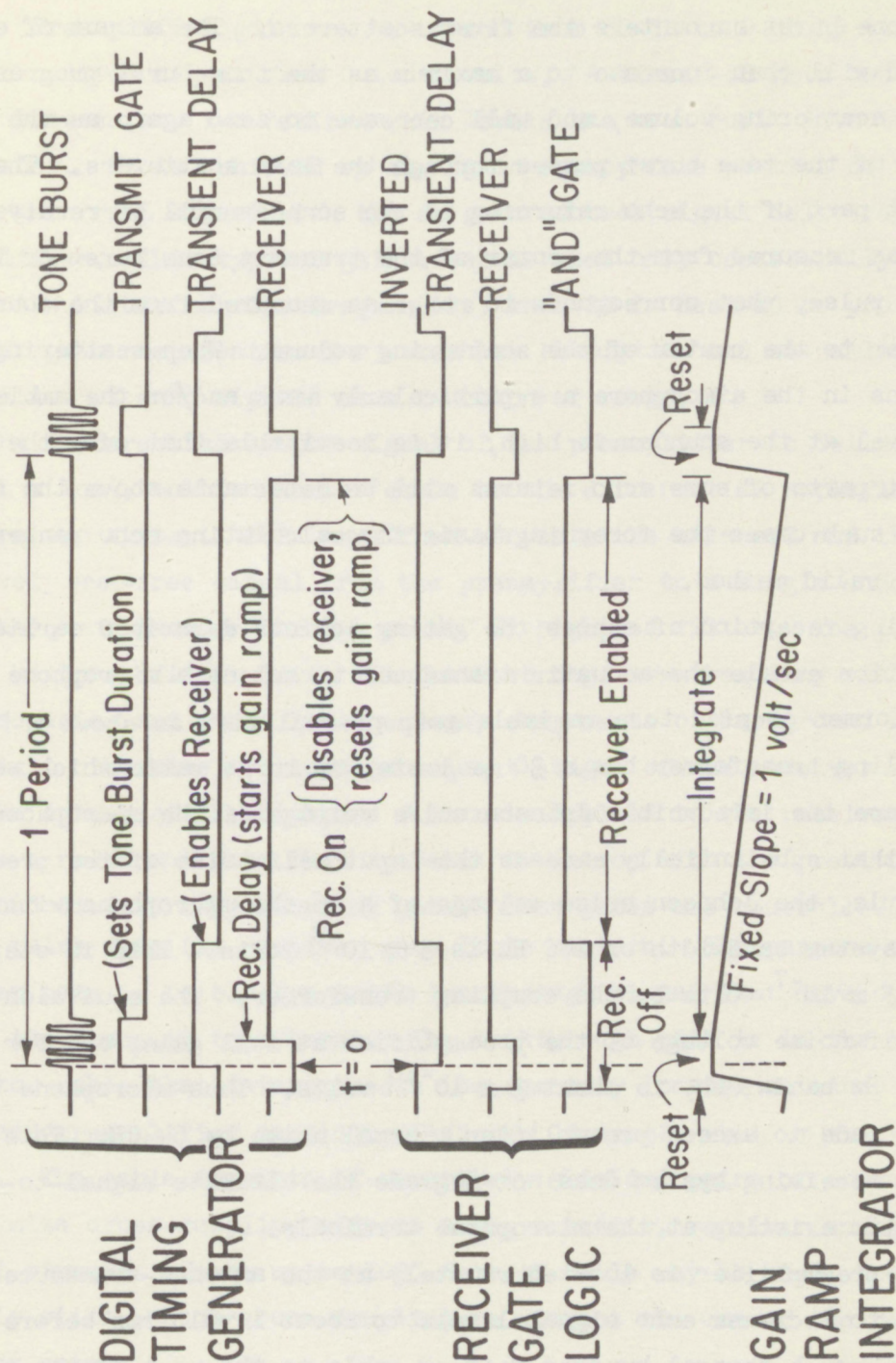


Figure 14. Mark II Echo Sounder Control Signals.



scattered weakly from the lower parts of the volume as the leading edge of the tone burst encounters the first scatterers. The amount of energy scattered will then increase to a maximum as the tone burst progresses into the scattering volume, and will decrease to zero again as the trailing edge of the tone burst passes through the last scatterers. The strongest part of the echo returning to the sounder will be received at a time, as measured from the center of the transmit tone burst or transmit gate pulse, that corresponds to range as measured from the sounder transducer to the center of the scattering volume. When scattering conditions in the atmosphere are particularly weak and/or the ambient noise level at the sounder is high, it is inevitable that only the strongest parts of some echo returns will be detectable above the ambient. In such cases the foregoing basis for calculating echo ranges is the only valid method.

During reception of echoes the gating actions described earlier in this section enable the acoustic transducer to act as a microphone which is transformer coupled to a variable-gain preamplifier as shown in figure 13. The coupling transformer has a 30 to 1 step-up turns ratio which serves to increase the irreducible Johnson noise voltage of the microphone to a level that substantially exceeds the input self-noise of the preamplifier. For example, the Johnson noise voltage of a 16-ohm microphone within a typical system bandwidth of 100 Hz is  $5 \times 10^{-9}$  volts. This is stepped up to  $1.5 \times 10^{-7}$  volts by the coupling transformer. The equivalent input self-noise voltage of the preamplifier at full gain, and for the same 100 Hz bandwidth, is about  $3 \times 10^{-10}$  volts. Thus microphone thermal noise is made to exceed preamplifier thermal noise by 54 dB. This insures that the receiving system does not degrade the ultimate signal-to-thermal noise ratio existing at the microphone terminals.

The preamplifier is located remotely at the antenna-transducer site in order to increase echo signal levels to about 1 volt rms before transmission through several hundred feet of cable to the rest of the receiver system. For this reason, the preamplifier includes a calibrated, remote



gain control subsystem and a balanced, low-impedance, differential output stage. Preamplifier gain may be varied from 60 dB to 0 dB by varying a dc gain control signal from 0 to +5 volts. A linear-dB gain sweep capability between any two desired gain levels has been built into the Mark II sounder. It is achieved by mixing an appropriate portion of the linear gain ramp signal with the dc gain control signal delivered to the preamplifier. This type of gain sweep is used only occasionally, however, and at the higher carrier frequencies, when it is desired to provide receiver gain compensation for molecular absorption and so-called excess attenuation of echo signals as a function of range.

The differential output signal of the preamplifier is delivered through a long, multiconductor cable to the differential amplifier of the receiver system. This amplifier converts the balanced and therefore relatively hum-free signal from the preamplifier to a single-ended signal for subsequent passage through an 800 Hz highpass filter. The purpose of the highpass filter is to eliminate strong, low-frequency wind noise, man-made noise and other low-frequency components of background noise that might otherwise overload subsequent stages of the receiver system.

The output of the highpass filter is applied to the receiver gate. This is a redundant gate that operates in unison with the previously described diode bridge shorting gate. Both gates are controlled by the output pulse from the receiver gate logic section. The purpose of the receiver gate is to block a small leakthrough signal that develops during the transmit tone burst. The leakthrough path is in the multiconductor cable that interconnects the remotely located antenna, transducer and preamplifier sections of figure 13 to the rest of the sounder system. The cable consists of separately shielded pairs of conductors to minimize cross-coupling effects among transmit, receiver and gate control signals. Since up to 1000 feet of cable may be used, however, there is still enough cross-coupling to warrant the use of the redundant receiver gate.



The echo signal from the receiver gate is applied to one of the two inputs of the  $1/R$  analog multiplier. The other input to the multiplier is a linear ramp signal generated by the gain ramp integrator. The output of the  $1/R$  analog multiplier at any time is simply one tenth the product of the applied echo signal and the instantaneous amplitude of the linear ramp. The linear ramp from the integrator always starts at zero volts dc and grows with time at the rate of 1 volt/sec. This causes the multiplier to act as an echo signal amplifier the gain of which periodically starts at zero and increases linearly with time at the rate of 0.1/sec. By the end of a 10 second echo receiving period, for example, the gain of the  $1/R$  analog multiplier has been swept from zero to unity. This type of gain sweep compensates for the spherical divergence or spreading loss of acoustic echoes as they are received from progressively longer ranges. The gain is varied inversely with range ( $1/R$ ) rather than as the inverse square of range ( $1/R^2$ ) because the output signal of the receiving transducer is proportional to acoustic pressure rather than acoustic power.

The basis for the start and reset timing of the gain ramp integrator was described earlier, and the gain ramp waveform relative to the transmit tone burst and various gate timing signals is shown in figure 14. The gain ramp integrator itself is a solid-state, commercially-available module that includes a gated operational amplifier. The operational amplifier section was converted to a linear integrator by the addition of a 2 uF feedback capacitor and a resistance that was adjusted to produce the desired integration rate of 1 volt/sec. The gate control of the module is connected to the aforementioned start and reset timing signal from the digital timing generator.

The range-compensated echo signal from the  $1/R$  analog multiplier is applied to the input of the tuned receiver. The receiver is constructed so that the center of its pass band automatically coincides with the frequency of an integral BFO that is the source of carrier frequency for the Mark II sounder. The receiver tuning is thus locked to the mean frequency of the echo signal. Receiver bandwidth is adjust-



adjustable and is normally set to accomodate just the major sidebands of the transmitted tone burst in order to achieve an optimum S/N with minimal loss of resolution. For example, a bandwidth of 100 Hz generally has been used for tone bursts lasting 20 msec, whereas a bandwidth of 10 Hz has been used for tone bursts of 200 msec and longer.

The tuned receiver has two outputs. One of these is an amplified replica of the echo signal as bandwidth-limited by the receiver tuned circuits. This is the type of signal that will be used for determining Doppler shifts of frequency between a transmitted tone burst and its received echo. It is planned to digitize this signal (and others) before recording in order (1) to eliminate frequency errors associated with analog tape recorder wow and flutter, and (2) to shorten the number of steps required for subsequent digital data analysis. The digital recording scheme, though not yet completed, is shown connected to the echo signal output of the tuned receiver on figure 13. The other output of the tuned receiver is the detected level of the echo signal. This is a fluctuating dc signal the amplitude of which is proportional to the acoustic pressure of echoes received after correction for spherical divergence. This signal is displayed as functions of range and time of day by means of the facsimile recorder.

### 3.2 Sidelobe Radiation

Data for plotting polar diagrams of an acoustic antenna having a physical aperture diameter of 4 feet were obtained outdoors at frequencies of 1, 2, 3, 4 and 5 kHz. The antenna tested was a fiberglass horn-reflector type in which acoustic energy from a transducer was coupled through a conical horn to a parabolic reflecting surface. Thus, the parabolic surface radiated a collimated beam of acoustic energy into the atmosphere. The extent of collimation and unwanted sidelobe radiation associated with it can be displayed graphically with polar diagrams. To obtain the necessary data two of the horn-reflector antennas were placed 100 feet apart, well away from reflecting structures. One antenna was rotated in azimuth as it radiated a constant acoustic power level. The signal level received



by the other antenna was simultaneously recorded as a function of transmitting antenna azimuth.

Although the antennas were elevated about 10 feet above the terrain and there was further depression of the terrain between the antennas, there were nonetheless some ground-reflection effects present. The standing waves produced by these reflections were studied by probing the line-of-sight path between the antennas with a sound level meter. The maximum fluctuation of sound pressure level along the path was about 6 dB. It was decided to accept that much fluctuation since even greater amounts had been measured during an earlier experiment which involved transmitting across a ravine. Wind and temperature effects sometimes produced very large fluctuations in received signal level. In high winds these fluctuations were often as much as 20 dB. Accordingly data were recorded only during calm or near-calm conditions in order to minimize meteorological effects.

The results of the measurements are presented in the polar diagrams of figure 15. The important sidelobes to consider (for vertical sounding) lie in the range of  $70^{\circ}$  to  $90^{\circ}$  from the main lobe. The  $20^{\circ}$  spread is to allow for atmospheric refraction of sound rays during strong temperature inversions. Under such conditions, sound radiated in a sidelobe  $20^{\circ}$  above the horizontal could be refracted downward to intersect the earth within operating range of the echo sounder. This would produce strong, unwanted echoes from terrain features and might also produce an unacceptable level of noise pollution if the sounder were located in a residential community. Considering the maximum sidelobe radiation levels at angles of  $70^{\circ}$  to  $90^{\circ}$  from the main lobe, figure 15 indicates that sidelobe suppression is about 25 dB at 1 kHz, 35 dB at 2 kHz, 37 dB at 3 kHz, 40 dB at 4 kHz and 45 dB at 5 kHz.

The on-axis sound pressure level was measured at various frequencies for the above antenna at a range of 100 feet from the aperture. The antenna was driven by an Altec Lansing 291-16A transducer with 40 watts of electrical input. The measured sound pressure levels were 104 dB



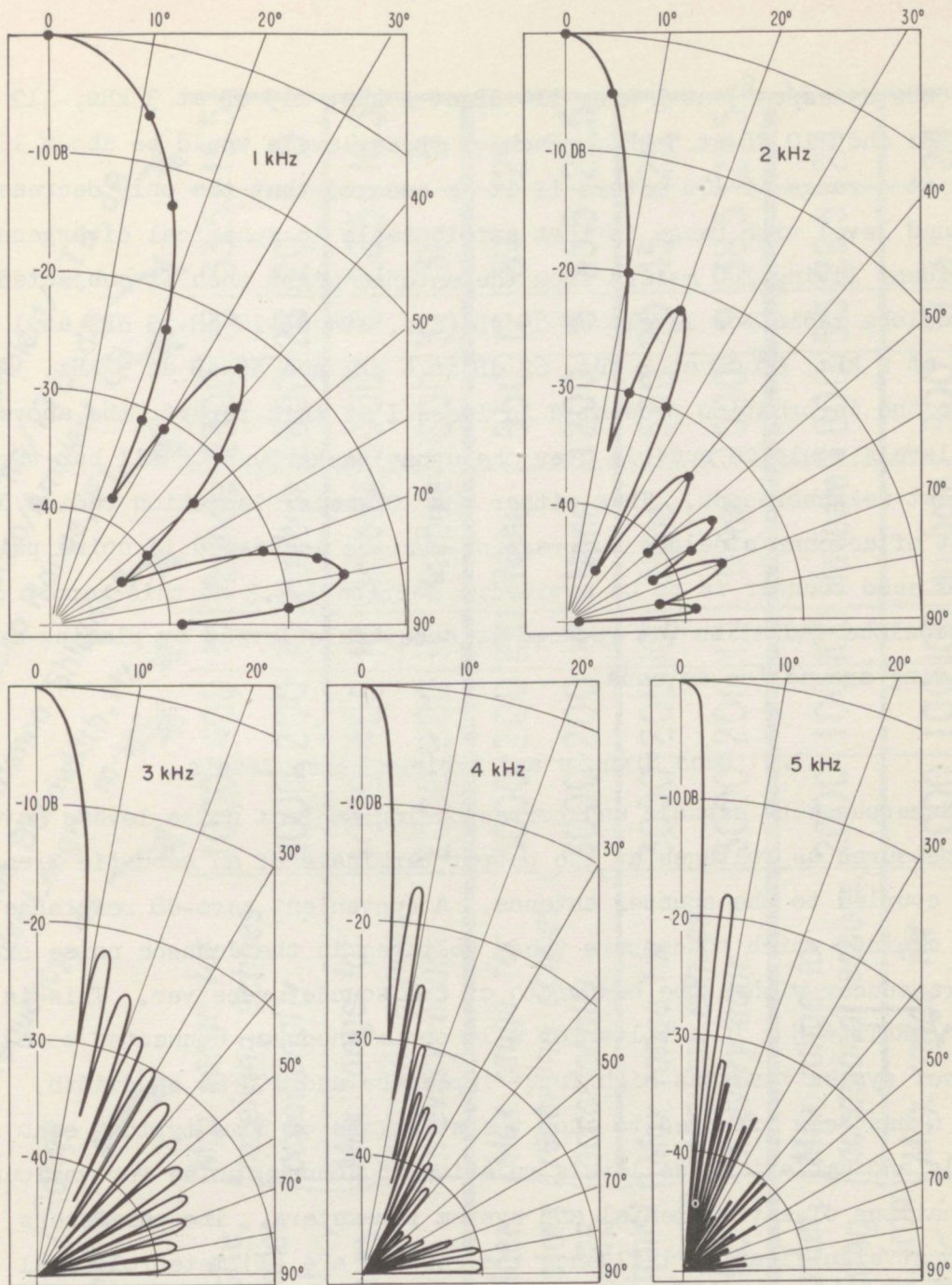


Figure 15. Polar diagrams of the gain pattern of the horn-reflector acoustic antenna.



(re .0002 dynes/cm<sup>2</sup>) at 1 kHz, 114 dB at 2 kHz, 115 dB at 3 kHz, 112 dB at 4 kHz and 110 dB at 5 kHz. Each of these levels would be about 10 dB lower at a range of 100 meters if it is assumed that the only decrease of sound level with range is that attributable to spherical divergence. A resident living 100 meters from the antenna might then be subjected to sidelobe radiation levels of 69 dB (i.e. 104 dB-10 dB-25 dB) at 1 kHz, 68 dB at 2 kHz, 68 dB at 3 kHz, 62 dB at 4 kHz and 55 dB at 5 kHz. According to the information presented in Phase I of this report, the above sidelobe levels would be audible over the urban background of all but the noisiest neighborhoods. Thus either the 100-meter isolation radius or the amount of antenna sidelobe suppression must be increased if noise pollution by the echo sounder is to be avoided. Section 3.3.3 of this report describes how sidelobe radiation was reduced to acceptable levels by placing anechoic shielding around the antenna.

### 3.3 Echo Signals and Ambient Noise Levels

Numerous echo signals and corresponding ambient noise levels have been measured as voltages at the output terminals of an acoustic transducer coupled to the sounder antenna. A convenient zero-dB reference level against which to compare these voltages is the Johnson noise of the transducer within the bandwidth of the sounder receiver. This is  $E_n = \sqrt{4RkTB} = 5 \times 10^{-9}$  volts for a 16 ohm transducer connected to a receiver system that has high input impedance and 100 Hz bandwidth. Table 6 has been prepared to show the strengths of some typical echo signals and ambient noise levels relative to Johnson noise for various combinations of environmental and system parameters. The parameters that most significantly influence the results are (1) meteorological conditions, (2) location (urban or rural), (3) antenna characteristics (gain, beamwidth and sidelobe suppression), (4) carrier frequency, (5) pulse length-receiver bandwidth combination, (6) radiated acoustic power and (7) echo dependability requirements (e.g. the percentage of time per hour throughout the day that one requires the reception of echo signals at or above a specified ratio of signal to ambient noise).



Table 6. Echo Signal and Ambient Noise Levels Relative to kTB Noise.

Echo Reliability / Range Relationship		Frequency, Hz	Pulse Length, m-sec	Antenna Bandwidth, Hz	Echo Shielding	Echo Range, Ft.	Echo/Ambient, dB	Ambient/kTB, dB		
LOCATION										
1.	Erie field site, rural, 15 miles east of mts.,	Max. range for receiving echoes occasionally.	1000	400	10	Haybale	5300	18	33.5	15.5
2.	on the plains, no trees.		2000	200	10	Haybale	2800	20	20	0
3.	Urban Boulder, roof of 6-story NOAA bldg., 25 ft. from exhaust fans, 100 ft. from heavy traffic.	Max. range for receiving echoes occasionally.	1000	400	10	Haybale	3000	8	26.5	18.5
4.	Urban Boulder, NOAA parking lot, 400 ft. from heavy traffic.		2000	200	10	Haybale	1600	31	31	0
5.	Urban Boulder, NOAA parking lot, 400 ft. from heavy traffic.	Max. range for frequent echoes in every hour.	3000	200	100	None	850	12	37	25
6.	Urban Boulder, NOAA parking lot, 400 ft. from heavy traffic.		3000	200	10	None	1200	6	35.5	29.5
7.	Urban Boulder, NOAA parking lot, 400 ft. from heavy traffic.	Max. range for frequent echoes in every hour.	3000	200	100	None	500	20	45	25
8.	Urban Boulder, NOAA parking lot, 400 ft. from heavy traffic.		3000	200	10	None	1000	9	38.5	29.5
9.	Urban Boulder, NOAA parking lot, 400 ft. from heavy traffic.	Max. range for occasional echoes.	2000	100	100	Haybale	1800	5.5	29.5	24
10.	Urban Boulder, NOAA parking lot, 400 ft. from heavy traffic.		2000	100	100	Haybale	900	9	33	24

SAMPLE N°



It can be seen from Table 6 that there are not yet enough data to show in complete detail the isolated effects on system performance of each of the seven parameters just mentioned. A superficial or first-cut assessment has been made, however, and this is presented below. The tentative and incomplete nature of this assessment is emphasized. A more comprehensive and accurate analysis than the one based on Table 6 will require the acquisition simultaneously of appropriate meteorological and echo sounding data to be obtained while varying each controllable parameter through a systematic schedule of values.

### 3.3.1 Meteorological Conditions

Wind and wind shear at and near the surface normally produce most of the ambient noise sensed by echo sounders except in urban, industrial and other populated areas where man-made noise often exceeds the natural ambient. High surface winds not only increase ambient noise over broad areas of terrain but also generate localized hydrodynamic and acoustic noise along the surfaces of sounder antennas unless the antennas are somehow protected from the wind. Placing an antenna in a pit with aperture flush to the surface reduces locally generated noise, as does the use of wind screens and shielding around the antenna. Temperature and velocity inhomogeneities in the atmosphere from just above the surface to the range limit of the sounder system determine the scattering cross sections (signal strengths) and structural patterns of echoes received. The wind shear and turbulence that produce the scattering phenomena may in themselves generate enough acoustic energy to contribute significantly to the ambient noise sensed by a sounder antenna, however, an evaluation of this possible contribution has not yet been completed.

Table 6 which summarizes data acquired during conditions of low surface winds (less than 5 knots), shows that the spectrum of ambient acoustic noise falls off sharply as frequency increases. For example, the ratio of ambient to kTB noise in a rural area is 15.5 dB lower for sample 2 at 2000 Hz than it is for sample 1 at 1000 Hz. Similarly the



ratio is 18.5 dB lower for sample 4 at 2000 Hz than it is for sample 3 at 1000 Hz. The 3 dB discrepancy between the spectral slopes of these two examples probably is due to slight changes in wind conditions and corresponding small changes in ambient noise level that occurred during the measurements.

The remarkably steep slope of the spectrum of ambient noise as measured with the sounder system is somewhat misleading. Part of the slope is indeed due to the actual spectrum of natural acoustic background, perhaps as much as 6 to 10 dB/octave. Part of the slope also may be due to local hydrodynamic pressure fluctuations generated by interaction of the wind with antenna surfaces. The spectral slope of hydrodynamic noise is about 12 dB/octave. A significant part of the slope as measured, however, must be attributed to the frequency-sensitive sidelobe response of the sounder antenna. A glance at the polar diagrams of figure 15 shows that the sidelobe response at off-axis angles of 70 to 90 degrees is roughly 10 dB lower at 2000 Hz than it is at 1000 Hz. Although these polar diagrams were obtained with an unshielded reflector-horn antenna, an anechoically shielded antenna should display somewhat similar side-lobe-vs-frequency characteristics.

Unfortunately there are not enough data in Table 6 to show the shape of the spectrum of ambient noise over a broad echo sounding frequency range of say 500 to 5000 Hz, and there are no quantitative meteorological data to show how the ambient noise level at a given frequency varies with the speed of surface and near-surface winds. It is planned to acquire such data systematically during the next phase of this work.

### 3.3.2 Location

The effect of location (urban-vs-rural) on echo sounder performance can be estimated from Table 6 for a sounder operating at a carrier frequency of 2000 Hz with an anechoically shielded antenna by comparing sample 2 (rural site near Erie, Colorado) with sample 9 (urban site in Boulder, Colorado). These samples show the maximum ranges from which



echoes were received, albeit infrequently. The ranges were 2800 feet at Erie and 1800 feet in urban Boulder. Adjustments must be made for differences in pulse length and receiver bandwidth before comparing the respective signal-to-ambient noise ratios of the two samples. If the receiver bandwidth of sample 9 were reduced from 100 Hz to the 10-Hz bandwidth of sample 2, the ambient and kTB noise levels of sample 9 would be reduced by 10 dB each (assuming a reasonable flat noise power spectrum for the bandwidth considered). Similarly if the pulse length of sample 9 were doubled to equal the pulse length of sample 2, the echo power received from a given volume of scatterers would increase 3 dB. Thus the adjusted echo-to-ambient noise ratio for sample 9 would be 18.5 dB compared to 20 dB for sample 2. These S/N's differ by only 1.5 dB, and for practical purposes may be considered to be roughly equal. One can then say that when echo sounding with a high-gain, anechoically-shielded antenna at 2000 Hz, radiating 200-m sec pulses at 8 acoustic watts, and receiving acoustic energy only within a bandwidth of 10 Hz centered on 2000 Hz, occasional echoes will be recorded at a signal-to-ambient noise ratio of about 20 dB from maximum ranges of 1800 feet in urban areas and 2800 feet in rural areas.

### 3.3.3 Antenna Characteristics

One of the major design goals for both the Mark I and Mark II sounders has been to achieve echo S/N's that, under rare conditions of negligible acoustic ambient or environmental background noise, are limited only by the irreducible Johnson or thermal noise of the antenna resistance. This design goal has been met. Samples 2 and 4 of Table 6, where the ratio of ambient to kTB noise is shown as 0 dB, are examples of sounder performance limited by the thermal noise of the receiving antenna. It is in fact possible that the ambient noise level might have been less than the kTB noise for these examples, and that is just the point, i.e. that the inherent thermal noise of the receiving antenna has set a limit on the smallest signal that the Mark II sounder can detect.



There are three interrelated areas within which future design improvements might make it possible for an echo sounder to detect smaller signals than those indicated by samples 2 and 4 of Table 6. These areas all have to do with improvements in antenna characteristics rather than improvements in the electronic circuits which follow the antenna. The areas involve (1) an increase in the forward (main lobe) gain of the antenna relative to an isotropic receiver (2) further suppression of antenna sidelobe response, and (3) an increase in sensitivity of the transducer driven by the antenna. The brute-force method of making the antenna aperture ever larger is not likely to produce corresponding dependable increases in antenna gain because of acoustic wavefront distortions produced by wind and temperature fluctuations in the atmosphere. Furthermore, for any given carrier frequency, as antenna aperture size increases the main beam width decreases. A half-power beam width of less than about 4 or 5 degrees probably is not desirable since the strong refracting effects of temperature and wind gradients in the atmosphere may cause backscatter wavefronts to return at angles up to several degrees off the beam axis. Lastly and obviously, large-aperture antennas are usually not portable and are difficult and unwieldy to steer. For the above reasons, and because the polar diagrams of figure 15 indicate adequately narrow beamwidths at all frequencies above 1 kHz, it is concluded that the present antenna aperture diameter of 4 ft is near optimum.

It may be possible to achieve an effective increase in overall antenna-transducer system gain by improving the efficiency with which received acoustic energy is converted by the antenna transducer to an electrical signal. Figure 16 shows the overall receiving efficiency of both the Mark I and Mark II antenna-transducer systems when the antenna aperture is illuminated by a plane wave at an rms acoustic pressure of 1 dyne/cm<sup>2</sup>. Both systems utilize the same horn-reflector antenna. The Mark II system, however, employs an Altec-Lansing 291-16A transducer to achieve a flatter frequency response than was obtainable with the University ID-40 transducer associated with the Mark I system. Note that the



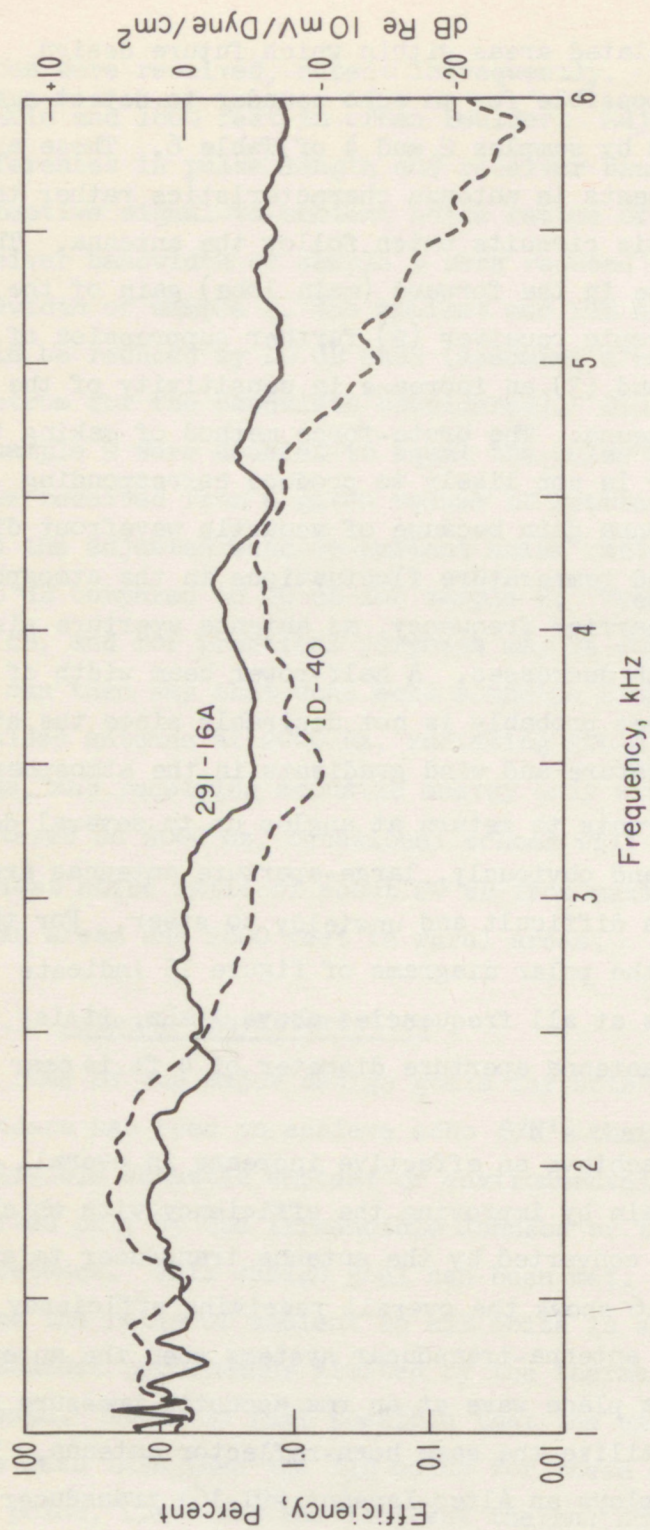


Figure 16. Receiving Efficiency of Transducers with Horn-Reflector Antenna.



ID-40 curve of figure 16 shows an efficiency peak of about 30% at a frequency of slightly less than 2 kHz. This peak was utilized extensively for echo sounding with the Mark I system. The ID-40 response falls off so rapidly with frequency, however, that satisfactory sounding records could not be obtained at frequencies above 3 kHz. A tradeoff was made, therefore, between the 2 kHz resonant peak of the ID-40 and the relatively flat frequency response of the 291-16A transducer. Consequently, excellent high resolution soundings of thermal plumes have been obtained with the Mark II system at carrier frequencies up to 5 kHz. Nonetheless, figure 16 shows that the overall receiving efficiency of the 291-16A transducer coupled to a horn-reflector antenna is only about 10% at frequencies up to 3 kHz, and declines with slight irregularities to about 1% at 5 kHz. It is hoped to increase the efficiency to about 50% at 2 kHz by carefully matching the throat impedance of the antenna to the acoustic input impedance of the transducer, and by further damping and stiffening of the antenna surfaces.

Figure 17 shows the overall transmitting efficiency of the Mark II antenna-transducer system when 1 watt rms of electrical power is applied to the 291-16A transducer. Efficiencies at this power level are, in general, above 50% at frequencies from 1 to 2 kHz, roughly 10% from 2 to 3.5 kHz, and roughly 3% at higher frequencies up to 6 kHz. These efficiencies, especially at the lower frequencies, are deemed to be satisfactory. Transmitting efficiencies, at any rate, are almost certain to improve automatically as the previously discussed improvements in receiving efficiency are achieved.

Further suppression of antenna sidelobe response appears to offer the most promise for increasing the ratio of echo signal to ambient noise when receiving, and for minimizing sidelobe radiation noise pollution levels when transmitting. First of all, it is obvious from the polar diagrams of figure 15 that sidelobes at angles of  $70^{\circ}$  to  $90^{\circ}$  from the main beam become progressively smaller as the echo carrier



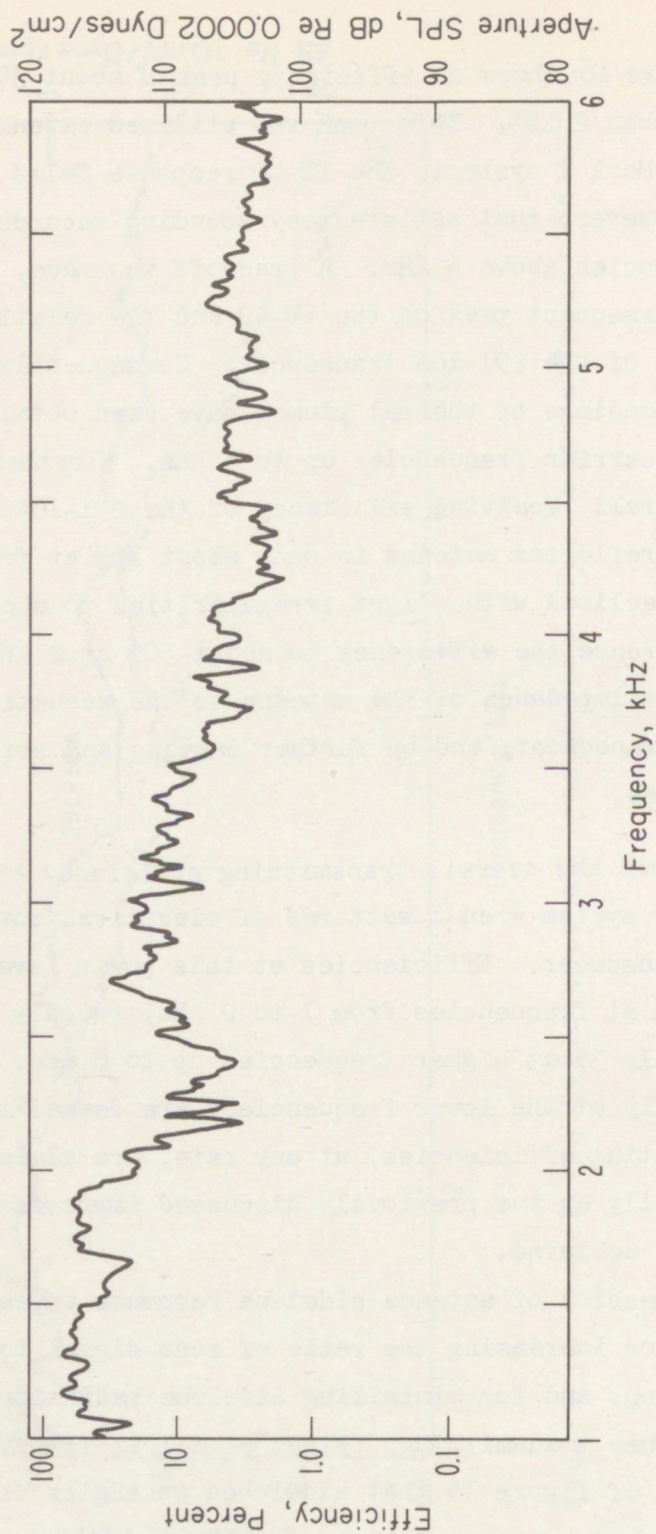


Figure 17. Transmit Efficiency of 291-16A Driver on Horn-Reflector Antenna.



frequency is increased. It is thus advantageous to use as high a carrier frequency as possible consistent with recognizing that absorption and excess attenuation losses increase severely with frequency.

An effective reduction of radiated sidelobes occurs as a direct consequence of transmitting tone bursts or pulses of acoustic power as opposed to CW transmissions. The sideband frequencies generated by tone bursting contribute to the resultant farfield polar response of a radiating aperture in a manner that results in a reduction of sidelobes without a corresponding broadening or weakening of the main beam response (Freedman, 1971, 1970, 1965). The pulse length must be short enough to limit the radiated carrier to bursts of a small number of cycles if the reduction in sidelobes is to be significant. It is planned to determine the reduction of sidelobe radiation as a function of pulse length for the Mark II antenna system.

A significant reduction of both radiated and received sidelobes has been achieved by constructing a semi-anechoic, semi-opaque shield around the Mark II antenna. Comparative measurements first were made of the  $90^\circ$  and  $80^\circ$  sidelobes radiated from (a) the unshielded Mark II horn-reflector antenna, and (b) the same antenna shielded by an admittedly crude anechoic structure of hay bales. The structure approximated an open-top cylinder with a diameter 3 times that of the 4 ft antenna aperture, and with a height extending to 2 aperture diameters above the antenna. The data obtained from these two sets of measurements are presented in Table 7. These data show that the anechoic shield provides a minimum improvement of 22 dB in suppression of the  $90^\circ$  sidelobe, and a minimum of 16 dB increased suppression of the  $80^\circ$  sidelobe at frequencies from 1 to 5 kHz.

Measurements were also made of the effectiveness of the anechoic shield in reducing the level of urban ambient acoustic noise received by the antenna. These data are also presented in Table 7. The results show an improvement of about 17 dB in noise rejection at frequencies from 1 to 3 kHz. The results also show only 6 to 7 dB of improvement at



Table 7. Anechoic Shield Antenna Sidelobe Reduction Data.

TRANSMITTING ANTENNA SIDELOBE DATA				
LEGEND	Frequency, hertz	dB re 0.0002 d/cm <sup>2</sup>		dB of improvement due to shielding, A-B
		Open antenna A	Shielded antenna B	
90° sidelobes at horizontal range of 180 feet for electrical input of 10 watts RMS	1000	75	47	28
	2000	66	44	22
	3000	60	32	28
	4000	62	30	32
	5000	50	26	24
80° sidelobes at slant range of 400 feet for electrical input of 10 watts RMS	1000	74	54	20
	2000	69	52	17
	3000	58	37	21
	4000	48	32	16
	5000	43	< 24	> 19

RECEIVING ANTENNA NOISE REJECTION DATA				
LEGEND	Frequency hertz	Receiver microvolts due to acoustic noise		dB of improvement due to shielding = 20 log (A/B)
		Open antenna A	Shielded antenna B	
Urban acoustic background monitored with antenna aimed vertically upwards	1000	1500	200	17.5
	2000	175	25	17.0
	3000	40	6	16.5
	4000	12	5	7.6
	5000	8	4	6.0



frequencies above 3 kHz. This is because the ambient noise at these frequencies was so much reduced by the shielding that it approached the irreducible thermal noise level of the antenna transducer.

The results of the "haybale" experiment were very encouraging. The additional 22 dB of radiated  $90^\circ$  sidelobe suppression, when added to the suppression values obtainable from the polar diagrams of figure 15, indicate that it will be safe to operate echo sounders in urban and suburban areas without creating a noise pollution problem. It is therefore planned to develop a mobile, steerable acoustic antenna with built-in anechoic shielding for use in populated areas.

### 3.3.4 Carrier Frequency

The optimum carrier frequency for achieving a given objective such as (1) high resolution of short-range echoes at good S/N's or (2) the acquisition of long-range echoes at some sacrifice in resolution and S/N, is determined by making tradeoffs between the group of factors that calls for high frequency as opposed to the group that calls for low frequency. The factors that call for high frequency are (1) increased antenna directivity, i.e., a narrower main-lobe beam width and smaller sidelobes at off-axis angles of  $70^\circ$  to  $90^\circ$ , (2) reduced response to ambient noise because of increased sidelobe suppression and also because of the characteristic spectrum of ambient noise which decreases in amplitude as frequency increases, (3) increased sensitivity to wind-produced Doppler shifts of echoes, since the magnitude of such shifts is directly proportional to carrier frequency, and (4) a slight increase with frequency of the strength of echoes from a turbulent atmosphere according to the  $\lambda^{-1/3}$  scattering law (Little, 1969). The factors that call for using a low carrier frequency are (1) reductions in molecular absorption and so-called excess attenuation losses associated with the propagation of sound outdoors, these losses being strong functions of frequency, and (2) higher transmitting and receiving efficiencies at the lower echo sounding frequencies of 1 to 2 kHz as shown in figures 16 and 17 for high-quality, commercially-available acoustic transducers and antenna systems.



As already noted in section 3.3.1 the suppression of sounder system response to ambient noise is about 15.5 to 18.5 dB greater at 2000 Hz than it is at 1000 Hz according to data samples 1 through 4 of Table 6. This argues for choosing 2000 Hz in preference to 1000 Hz as a carrier frequency for producing echoes of very high S/N at short to medium ranges. Indeed the ratio of echo to ambient signal level in a bandwidth of 10 Hz centered about a 2000 Hz carrier frequency is 31 dB in sample 4 of Table 6. This excellent S/N is for echoes received from a range of only 1600 feet, however. Sample 1 of Table 6 shows what had to be done in order to receive echoes from a range of 5300 feet. The carrier frequency had to be lowered to 1000 Hz and the pulse length doubled to 400 msec in order to receive signals at an echo-to-ambient ratio of only 18 dB. If the carrier frequency had not been thus lowered, molecular absorption and excess attenuation losses at 2000 Hz would have limited the maximum range for receiving occasional echoes to about 2800 feet as illustrated by sample 2 of Table 6.

### 3.3.5 Pulse Length-Receiver Bandwidth

The spatial or range resolution of acoustic echo returns is inversely proportional to transmitted pulse length. For example, range resolution is about 11 feet when the sounder is set to transmit 20 msec tone bursts, and 110 feet for 200 msec tone bursts. Thus, it is desirable, in the interests of obtaining high-resolution sounding records, to use the shortest pulse length possible consistent with receiving echo returns at acceptable S/N's. If, on the other hand, a particular application dictates that receiving echoes at high S/N's is more important than high resolution, it then becomes desirable to use the longest pulse length possible consistent with recording echo patterns at acceptable degrees of resolution, since the amount of echo signal energy received is directly proportional to pulse length. In short, to decide what pulse length to use, one must make the usual tradeoff between resolution and the S/N desired at some specified maximum range.



In an optimally adjusted system the received  $S/N$  increases with pulse length not only because of a proportionate increase in transmitted energy, but also because of a permissible proportionate decrease in receiver bandwidth. The latter accomplishes a reduction of received noise without a corresponding reduction of received signal. Receiver bandwidth of the Mark II sounder is normally set to twice the reciprocal of the transmitted pulse length in order to accommodate the received carrier and just those upper and lower sideband frequencies that fall within the first loop of the  $\sin x/x$  type of spectral envelope characteristically generated by the act of pulsing. This achieves a favorable compromise between high  $S/N$  (associated with narrow-bandwidth reception), and high-fidelity reproduction of received echo pulses (associated with broad-bandwidth reception). When echo sounding with extremely long pulse lengths, however, bandwidths narrower than 10 Hz are never employed, since wind-produced Doppler shifts of several Hz might otherwise cause some echo returns to fall outside the tuned pass band of the receiver. Thus, sample 1 of Table 6 shows that a pulse length of 400 msec was employed in order to radiate a relatively large amount of acoustic energy into the atmosphere in an effort to receive echoes from a range of about one mile. This pulse length calls for an optimum receiver bandwidth of 5 Hz, but a bandwidth of 10 Hz was instead used to allow for possible Doppler shifts in the echo returns.

### 3.3.6 Radiated Acoustic Power

The Mark II Echo Sounder employs a horn-reflector antenna driven by a high-quality public-address type acoustic transducer. The transmitting efficiency of this combination, as shown by figure 17, varies from about 50% at frequencies of 1 to 2 kHz to about 3% at frequencies from 4 to 6 kHz. The electrical power applied to the transducer is 40 watts rms at all frequencies, so that the radiated acoustic power varies from 20 watts to 1.2 watts as a function of frequency, - a power level variation of about 12 dB. It will, of course, be desirable to reduce this variation as much as possible through improvements in antenna and antenna-transducer coupler



designs. It is emphasized that higher acoustic transmission efficiency is to be found by improving the coupling between transducer and antenna and by increasing the damping, stiffening, etc of the antenna surfaces. The transducer itself has already been evaluated by comparison with other commercially available transducers in a series of frequency response tests. The results of these tests are shown in figure 18. Each transducer was in turn coupled to a small, rigid-walled horn and driven by 1 watt of electrical power while the on-axis sound pressure level was measured 1 foot from the mouth of the horn as a function of frequency. The curves of figure 18 show that the type 291-16A transducer has an output that is flat, within  $\pm 2$  dB from about 1 to 6 kHz. The type 808-16A has an equally flat response curve but its electrical power rating is only 20 watts rms, whereas the 291-16A is rated at 40 watts. On the basis of the response curves of figure 18 it is concluded that either the 291-16A transducer or a 100 watt version of the same transducer (not shown) will furnish ample acoustic power to a properly designed coupler and antenna system within the echo sounder frequency range of 1 to 6 kHz. It seems unlikely that more acoustic power than is available from these transducers will be needed or desired. For one thing, finite-amplitude acoustic wave propagation would occur within the antenna at significantly higher power levels. This would result in the production of undesired harmonics of the carrier frequency and, probably, a degradation in antenna performance. For another thing, sidelobe radiation levels from the antenna would exceed the noise pollution criteria developed in Phase I of this report unless additional sidelobe suppression were provided to offset the effects produced by a substantial increase in radiated power.



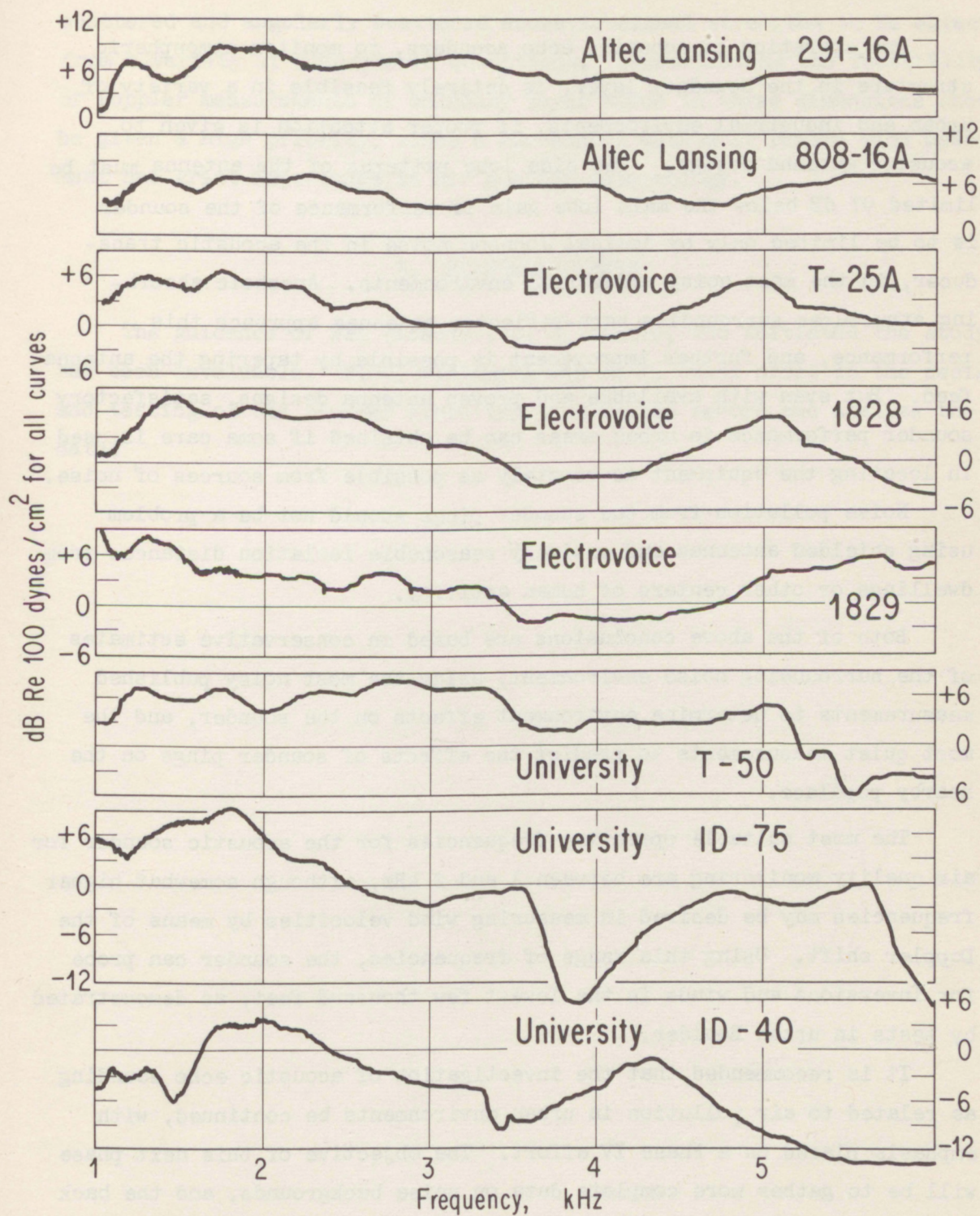


Figure 18. Frequency Response Comparison of Different Transducer.



#### 4. CONCLUSIONS

The operation of acoustic echo sounders, to monitor atmospheric structure in the boundary layer, is entirely feasible in a variety of urban and industrial environments, if proper attention is given to acoustic antenna design. The side lobe patterns of the antenna must be limited 97 dB below the main lobe gain if performance of the sounder is to be limited only by nominal Johnson noise in the acoustic transducer, in the most noisy industrial environments. Anechoic absorbing structures surrounding horn-reflector antennas approach this performance, and further improvement is possible by tapering the antenna feed. But even with available and proven antenna designs, satisfactory sounder performance in urban areas can be obtained if some care is used in locating the equipment as remotely as possible from sources of noise.

Noise pollution from the sounder pings should not be a problem using shielded antennas and entirely reasonable isolation distances from dwellings or other centers of human activity.

Both of the above conclusions are based on conservative estimates of the surrounding noise environment, using the most noisy published measurements to determine environment effects on the sounder, and the most quiet measurements to predict the effects of sounder pings on the nearby populace.

The most suitable operating frequencies for the acoustic sounder for air quality monitoring are between 1 and 2 kHz, although somewhat higher frequencies may be desired in measuring wind velocities by means of the Doppler shift. Using this range of frequencies, the sounder can probe for inversions and winds in the lowest few thousand feet, as demonstrated by tests in urban Boulder.

It is recommended that the investigation of acoustic echo sounding as related to air pollution in urban environments be continued, with emphasis placed on a Phase IV effort. The objective of this next phase will be to gather more complete data on noise backgrounds, and the back



scattered and angularly scattered acoustic signal strengths to be expected from a variety of atmospheric conditions. Demonstrating the feasibility of Doppler measurements of boundary layer winds in three dimensions should be given a high priority, since a successful method of remote wind measurement has great importance in air quality meteorology.

## 5. ACKNOWLEDGMENTS

The guidance of WPL Director, C. G. Little, who initiated the study, has been invaluable. B. C. Willmarth and E. J. Owens aided in the design and testing of the sounder circuitry, and helped record and analyze the data.



## 6. REFERENCES

- Bateman, W. F., and E. Ackerman (1955), Some observations on small town noise, Noise Control 1, (6) 40.
- Beran, D. W., R. M. Reynolds, and J. T. Gething (1970), Sound attenuation in the free atmosphere, Project EAR Report V, Meteorology Dept. Univ. of Melbourne, Australia, p. 64.
- Berendt, R., D., G. E. Winzer, and C. B. Burroughs (1967), A guide to airborne, impact, and structure borne noise-control in the multi-family dwellings, U. S. Dept. Housing & Urban Dev., Wash., D. C. C5-C12.
- Blazier, W. E., Jr. (1968), Criteria for control of community noise, Sound and Vibration 2 (5), 11-18.
- Bonvallet, G. L. (1951), Levels and spectra of traffic, industrial, and residential area noise, J. Acoust. Soc. Amer. 23, 435-439.
- Delsasso, L. P, and R. W. Leonard (1953), Attenuation of sound in the atmosphere, UCLA Rept. on Contr. W28 (099) ac 228, 62 pp.
- Evans, E. J., and E. N. Bazley (1956), The absorption of sound in air at audio frequencies, Acustica 6, 238-245.
- Fletcher, H. (1940), Auditory patterns, Rev. Mod. Phys. 12, 47-65.
- Freedman, A. (1971), Farfield of pulsed rectangular acoustic radiator, J. Acoust. Soc. Amer. 49, 738-748.
- Freedman, A. (1970), Sound field of plane or gently curved pulsed radiators, J. Acoust. Soc. Amer. 48, 221-227.
- Freedman, A. (1965), Sound field of a pulsed plane transducer, U. S. Navy Electron. Lab., Rept. 1304, San Diego, Calif.
- French, N. R., and J. C. Steinberg (1947), Factors governing the intelligibility of speech sounds, J. Acoust. Soc. Amer. 19, 90-119.
- Garner, W. R. (1947), Auditory thresholds of short tones as a function of repetition rates, J. Acoust. Soc. Amer. 19, 600-608.
- Harris, C. M. (1966), Absorption of sound in air versus humidity and temperature, J. Acoust. Soc. Amer. 40, 148-159.
- Harris, C. M. (1963), Absorption of sound in air in the audio-frequency range, J. Acoust. Soc. Amer. 35, 11-17.



- Harris, C. M., and W. Tempest (1964), Absorption of sound in air below 1000c.p.s., J. Acoust. Soc. Amer. 36, 2390-2394.
- Hawkins, J. E., Jr., and S. S. Stevens (1950), The masking of pure tones and of speech by white noise, J. Acoust. Soc. Amer. 22, 6-13.
- Henderson, M. C., A. V. Clark, and P. R. Lintz (1965), Thermal relaxation in oxygen with H<sub>2</sub>O, HDO, and D<sub>2</sub>O vapors as impurities, J. Acoust. Soc. Amer. 37, 457-463.
- Kryter, K. D., and K. S. Pearsons (1963), Some effects of spectral content and duration on perceived noise level, J. Acoust. Soc. Amer. 35, 866-83.
- Little, C. G. (1969), Acoustic methods for the remote probing of the lower atmosphere, Proc. IEEE 57, 571-578.
- McAllister, L. G., J. R. Pollard, A. R. Mahoney, and P. J. R. Shaw (1969), Acoustic sounding - a new approach to the study of atmospheric structure, Proc. IEEE 57, 579-587.
- Munson, W. A. (1947), The growth of auditory sensation, J. Acoust. Soc. Amer. 19, 584-591.
- Nyquist, H. (1928), Thermal agitation of electric charge in conductors, Phys. Rev. 32, 110-113.
- Ostergaard, P. B., and R. Donley (1964), Background-noise levels in suburban communities, J. Acoust. Soc. Amer. 36, 409-413.
- Pierce, A. D. (Aug., 1966), Geometrical acoustics theory of waves from a point source in a temperature and wind-stratified atmosphere, Avco Corp. Rept. AVSSD-0135-66-CR, AFCRL-66-454, (AD 636 159).
- Robinson, D. W., and R. S. Dadson (1957), Threshold of hearing and equal-loudness relations for pure tones, and the loudness function, J. Acoust. Soc. Amer. 29, 1284-1288.
- Sivian, L. J. (1947), On hearing in water vs. hearing in air, J. Acoust. Soc. Amer. 19, 461-463.
- Stevens, K. N., W. A. Rosenblith, and R. H. Bolt (Jan., 1955), A community's reaction to noise: Can it be forecast? Noise Control 1 (1), 63-71.
- Stevens, S. S. (1961), Procedure for calculating loudness: Mark VI, J. Acoust. Soc. Amer. 33, 1577-85.
- Wescott, J. W., W. R. Simmons, and C. G. Little (Jan., 1970), Acoustic echo sounding measurements of temperature and wind fluctuations, ESSA ERLTM-WPL 5, 1-24.



## APPENDIX A

### DERIVATION OF THE NOISE FIGURE EQUATION

The ambient noise figure specifies the environmental noise received by the acoustic echo sounder relative to the lowest noise level that can be realized - the Johnson or thermal noise generated in the transducer element (Nyquist, 1928). Since the amount of environmental noise received is determined by the acoustic antenna, we define the relevant properties of the acoustic antenna before proceeding with the noise figure derivation.

The acoustic antenna is a directional antenna characterized by a main lobe along which the maximum acoustic power per unit solid angle is either transmitted or received. If cylindrical symmetry is assumed about the main lobe axis, any departures in direction from the main lobe axis can be described by the angle of transmittance or incidence,  $\theta$ , measured from the axis. Since the receiving mode is concerned here,  $\theta$  will be called the angle of incidence.

Usually the directional properties of an antenna are described by an antenna gain factor, a factor that relates the directional properties of an antenna to one that is isotropic. For experimental measurements it will be more convenient to use the antenna side lobe attenuation function  $\epsilon(\nu, \theta)$  to describe the directional characteristics of the antenna.  $\epsilon(\nu, \theta)$  is defined as the ratio of the rms voltage  $V(\nu, \theta)$  developed at the transducer terminals when monochromatic sound of frequency  $\nu$  and sound pressure  $p(\nu)$  is incident on the antenna from the direction  $\theta$ , to the rms voltage  $V(\nu, 0)$  developed at the transducer terminals when monochromatic sound of the same frequency and pressure is incident on the antenna along the main lobe ( $\theta = 0$ ), or

$$\epsilon(\nu, \theta) = \frac{V(\nu, \theta)}{V(\nu, 0)} \quad . \quad (A1)$$



Implicit in (A1) is the behavior of the side lobes and the effective antenna aperture with frequency and angle of incidence.

The noise figure is defined as

$$F \equiv 20 \log \frac{V_a(\nu, \theta)}{V_j}, \quad (A2)$$

where  $V_a(\nu, \theta)$  is the rms transducer output voltage that is developed when acoustic noise of rms sound pressure  $p(\nu, \theta)$  for a band width of one Hertz and at a frequency,  $\nu$ , is incident on the antenna from the direction  $\theta$ .

The rms noise voltage developed at the transducer output as a result of the Johnson noise generated in the transducer element,  $V_j$ , is written as

$$V_j^2 = 4kT\Omega \quad (A3)$$

for a band width of one hertz, where  $\Omega$  and  $T$  are the ohmic resistance and absolute temperature of the transducer element respectively and  $k$  is Boltzmann's constant ( $1.38 \times 10^{-23}$  Joules/ $^{\circ}$ K).

When (A1) and (A3) are substituted into (A2), the noise figure can be written in terms of the antenna-transducer parameters;

$$F - 20 \log \epsilon(\nu, \theta) = 20 \log V_a(\nu, 0) - 10 \log T - 10 \log 4k\Omega. \quad (A4)$$

The left side of (A4) involves the noise figure and the measurable side lobe attenuation factor. It remains to express the right hand side in terms of sound pressures of the noise existing at the antenna, pressures that would be measured by sound level meter measurements. The value  $V_a(\nu, 0)$  is the rms transducer terminal voltage developed when ambient noise in a band width of one hertz at the frequency,  $\nu$ , and rms sound pressure  $p(\nu, 0)$  is incident on the antenna along the main lobe. The acoustic antenna transducer efficiency,  $\alpha(\nu)$ , is measured under the same conditions with the



exception that a pure tone of frequency  $\nu$  is used instead of noise. If  $\alpha(\nu)$  is known, then the transducer voltage can be predicted when the sound pressure at normal incidence is known. Then

$$V_a(\nu, 0) = \alpha(\nu) p_a(\nu, 0) \quad . \quad (A5)$$

Substituting (A5) into (A4) gives

$$F - 20 \log \epsilon(\nu, \theta) = 20 \log p_a(\nu, 0) + 20 \log \alpha(\nu) - 10 \log T - 10 \log 4k\Omega \quad . \quad (A6)$$

Environmental noise is measured in terms of sound pressure levels (SPL) in decibels above the sound pressure for the average threshold of hearing: 0.0002 dynes per square centimeter ( $p_r$ ). Sound pressure levels measured in a band width of  $\Delta\nu$  Hertz can be reduced to sound pressure spectrum levels (SL), the sound pressure level  $p(\nu)$  (re 0.0002 dynes/cm<sup>2</sup>) for a one Hertz band width, by

$$SL = SPL - 10 \log \Delta\nu = 20 \log \frac{p(\nu)}{p_r} \quad . \quad (A7)$$

The desired expression is obtained by substituting (A7) into (A6) and the noise figure equation is written as

$$F - 20 \log \epsilon(\nu, \theta) = SL_a + 20 \log \alpha(\nu) - 20 \log p_r - 10 \log T - 10 \log 4k\Omega \quad , \quad (A8)$$

which involves the two quantities of interest on the left in terms of the independently measured quantities of the antenna, transducer, and environmental noise field. When the values for  $p_r$  and  $k$  are substituted into (A8) and considering a transducer whose ohmic resistance is 16 ohms, (A8) reduces to

$$F - 20 \log \epsilon(\nu, \theta) = 137 + SL_a + 20 \log \alpha(\nu) - 10 \log T \quad . \quad (A9)$$



## APPENDIX B

### DERIVATION OF THE ISOLATION RADIUS EQUATION

The intensity ( $I(\nu)$ ) of an acoustic wave at a distance  $r$  from a directional antenna is given by (ignoring absorption)

$$I(\nu) = \frac{P}{4\pi r^2} G(\theta, \varphi, \nu) \quad (B1)$$

where  $P$  is the total power radiated by the acoustic antenna and  $G(\theta, \varphi, \nu)$  is the gain factor relative to an isotropic radiator. The angles of elevation  $\theta$  and azimuth  $\varphi$  are measured with respect to the antenna main lobe axis.

The intensity level is related to the acoustic intensity by

$$IL = 10 \log \frac{I(\nu)}{I_r} \quad (B2)$$

in which  $I_r = 10^{-12}$  watts/meter<sup>2</sup> is the intensity sound at the threshold of hearing. By substituting (B1) and using the numerical values for the constants, the intensity level can be written as

$$IL = 109 + 10 \log P + 10 \log G(\theta, \nu) - 20 \log r \quad (B3)$$

If an atmospheric temperature and pressure of 25°C and one atmosphere respectively are assumed, the intensity level can be related to the sound pressure level by

$$SL = IL + 0.2 \cong IL \quad (B4)$$

Consequently, the sound pressure level of an acoustic wave at a distance  $r$  from the acoustic antenna is given by

$$SL = 109 + 10 \log P + 10 \log G(\theta, \nu) - 20 \log r \quad (B5)$$